WORKING NOTES ON THE TIME MINIMAL SATURATION OF A PAIR OF SPINS AND APPLICATION IN MAGNETIC RESONANCE IMAGING

B. BONNARD, O. COTS, J. ROUOT, AND T. VERRON

ABSTRACT. In this article, we analyse the time minimal control for the saturation of a pair of spins of the same species but with inhomogeneities of the applied RF-magnetic field, in relation with the contrast problem in Magnetic Resonance Imaging. We made a complete analysis based on geometric control to classify the optimal syntheses in the single spin case to pave the road to analyze the case of two spins. The `Bocop` software is used to determine local minimizers for physical test cases and Linear Matrix Inequalities approach is applied to estimate the global optimal value and validate the previous computations. This is complemented by numerical computations combining shooting and continuation methods implemented in the `HamPath` software to analyze the structure of the time minimal solution with respect to the set of parameters species.

1. INTRODUCTION

In Magnetic Resonance Imaging (MRI), a challenging problem is to maximize the contrast between two observed species, *e.g.* healthy tissues from tumors by saturating one of the species. Optimal control techniques were introduced in this domain in the eighties [17] and were developed very recently under the impulse of S. Glaser using advanced analytical and numerical techniques. This gave rise to a series of articles which analyze the contrast problem, starting from the ideal contrast problem where only a pair of spins is considered, to the optimal control of an ensemble of pairs of spins, taking into account the so-called B_0 and B_1 inhomogeneities [22, 23, 11, 8] to compute robust control. A first major contribution in this area was for some physical cases, the explicit computation of the time minimal control of saturating a single spin, that is steering the state representing the spin to zero and showing that the standard inversion sequence applied in practice is not optimal in many physical cases, *e.g.* the blood case [22]. Additional pulses have to be used corresponding to the so-called singular control [5]. This computation relies on an intense research activities at the end of the eighties to the computation of the time-minimal closed loop solution for $\mathcal{C}^\omega$-planar single input control system in a neighborhood of a given point, taking into account the Lie algebraic structure of the systems of this point [12, 35, 33, 34].

Thanks to the bilinear structure of the model, this local analysis can be globalized for a single spin and a first contribution of our article is to make a complete classification of the time minimal syntheses taking into account the time relaxation parameters of the species and the maximal amplitude of the applied RF-field (control). Our aim is to extend this analysis to the case of two spins in relation to the problem of the so-called B_1-inhomogeneity, that is of the applied RF-field. The analysis is very complex and we present a combination of algebraic and geometric methods based on [6] and adapted numerical schemes to analyze the problem implemented in specific software: `Bocop` [3], `HamPath` [15], `GloptiPoly` [19]. A similar analysis was presented for the contrast problem [11] but for this simplified version it is complete in many directions, thus providing a testbed of the methods to deal with the time minimal control of a single input control system where the state space is of codimension 4, depending upon 2-parameters and with many local optima.

This article is organized as follows. In section 2, we present the mathematical model, that is the Bloch equations [26] and we discuss the underlying optimal control problem in MRI, that is the contrast problem with B_0 and B_1 inhomogeneities [23], to introduce the time minimal saturation of a pair of spins, that we analyze in this article. The seminal result in optimal control theory is the Maximum Principle [31] which is recalled to select extremal curves candidates as minimizers. The extremal controls split into bang controls and the so-called singular controls whose role in the time minimal problem is recalled [7]. In section 3, the time minimal saturation of a pair of spins of the same species with B_1-inhomogeneities is investigated. A preliminary study concerning the case of a simple spin is presented in details using geometric control theory techniques. This led to a complete classification of the optimal syntheses to steer any state to the origin. Thanks to the symmetry of revolution it is reduced to a time minimal control problem for a single-input 2D-system. All the fine results of the geometric theory [13, 35] are used to provide a complete classification depending upon the physical parameters and completing [22]. The next step in section 4 is to extend this analysis to a pair of spins, numerical methods are used to complete the analysis. First of all, the direct methods implemented in the `Bocop` code are applied to analyze for physical cases: Desoxygenated and Oxygenated case, Cerebrospinal fluid and Water case. Global optimality is analyzed using LMI methods [24]. In the final part, the problem is analyzed using multiple shooting methods implemented in the `HamPath` software [15] and completed by numerical continuations (available in the software) to compute the optimal solutions for a continuous set of physical relaxation parameters. This numerical investigation, based on homotopy reveals the existence path of zeros that has to be compared to determine the global optimal. In section 5, we discuss the theoretical complexity of the procedure. The crucial point is to analyze the singular trajectories associated with a $4D$-Hamiltonian flow, with constraints and many singularities. They are computed using symbolic computations, extending techniques from [6]. They led to identify a simplified case corresponding to the so-called water case, important in practice and which is a generalization of the standard inversion sequence for a single spin. This case is important to analyze the general case, using homotopy methods.

2. Theoretical concepts and results

Name	T_1	T_2	$\frac{T_2}{T_1} = \frac{\gamma}{\Gamma}$	$\theta = \mathrm{atan}(\frac{\gamma}{\Gamma})$
Water	2.5	2.5	1.0	0.7854
Fat	0.2	0.1	0.5	0.4636
Cerebrospinal Fluid	2.0	0.3	0.15	0.1489
Oxygenated blood	1.35	0.2	0.1481	0.1471
White cerebral matter	0.78	0.09	0.1154	0.1148
Gray cerebral matter	0.92	0.1	0.1087	0.1083
Brain	1.062	0.052	0.0490	0.0489
De-oxygenated blood	1.35	0.05	0.0370	0.0370
Parietal muscle	1.2	0.029	0.0242	0.0242

TABLE 1. Matter name with relaxation times in seconds, ratio T_2/T_1 and value $\theta = \mathrm{atan}(\gamma/\Gamma)$.

2.1. **The model.** We consider an ensemble of spin-1/2 particules, excited by a radio-frequency (RF) field which is ideally assumed homogeneous, each spin of this ensemble being described by the magnetization vector $M = (M_x, M_y, M_z)$ whose dynamics is governed in a specific rotating frame by the Bloch equation [26]:

$$\dot{M}_x(t) = -\frac{M_x}{T_2} + \omega_y M_z,$$

$$\dot{M}_y(t) = -\frac{M_y}{T_2} - \omega_x M_z,$$

$$\dot{M}_z(t) = \frac{M_0 - M_z}{T_1} - \omega_y M_x + \omega_x M_y,$$

where T_1, T_2 are respectively the longitudinal, transversal relaxation constants, M_0 is the thermal equilibrium and $\omega = (\omega_x, \omega_y)$ is the control corresponding to the applied RF-magnetic field, with $\omega_{\max}$ the maximal amplitude of the control, *i.e.* $\omega_x^2 + \omega_y^2 \le \omega_{\max}^2$. Table 1 gives a list of longitudinal and transversal relaxation constants for the main practical cases.

Up to a renormalization of M introducing $(x, y, z) = (M_x, My, M_z)/M_0$ and a time reparameterization, the dynamics take the form:

$$\dot{x}(t) = -\Gamma x + u_y z,$$

$$\dot{y}(t) = -\Gamma y - u_x z,$$

$$\dot{z}(t) = \gamma(1 - z) - u_y x + u_x y.$$

In the relevant physical cases, one has $0 \le \gamma \le 2\Gamma$ and the Bloch ball: $x^2 + y^2 + z^2 \le 1$, is invariant for the dynamics. Thanks to the reparameterization, one can assume that the control is bounded by $u_x^2 + u_y^2 \le 1$. In this case, the relations between the

parameters (γ, Γ) and $(T_1, T_2, \omega_{\max})$ are the following:

$$(2.1) \qquad\qquad \gamma = \frac{1}{T_1\,\omega_{\max}}, \quad \Gamma = \frac{1}{T_2\,\omega_{\max}}.$$

The system admits a symmetry of revolution around the z-axis, which allows us to set $u_y = 0$ and to restrict each spin system to a single-input control system in the trace of the Bloch ball on the plane (y, z). The system then takes the form:

$$(2.2) \qquad\qquad \begin{aligned} \dot{y}(t) &= -\Gamma y - uz, \\ \dot{z}(t) &= \gamma(1 - z) + uy, \end{aligned}$$

with $u = u_x$, $|u| \leq 1$.

The <u>problem of saturation</u> associated to the contrast problem by saturation in MRI is to steer from the north pole $N = (0, 1)$ to the origin $O = (0, 0)$ one of the two species to be distinguished. In the contrast problem with RF-inhomogeneities, which is due to the spatial position of the species in the image, one has to consider an ensemble of pair of spins, such as for each system, the dynamics is perturbed. This perturbation is modeled as a rescaling of the maximal amplitude perceived by the spin. Restricting again to the sub-problem of saturation of one species, and considering only an ensemble of two pairs of spins, this leads to consider the case of a couple of systems (2.2) with the same parameters (γ, Γ) but with a distortion in the maximal amplitude, that is:

$$\begin{cases} \dot{y}_1(t) = -\Gamma y_1 - u\,z_1, \\ \dot{z}_1(t) = \gamma(1 - z_1) + u\,y_1, \end{cases} \qquad \begin{cases} \dot{y}_2(t) = -\Gamma y_2 - (1 - \varepsilon)\,u\,z_2, \\ \dot{z}_2(t) = \gamma(1 - z_2) + (1 - \varepsilon)\,u\,y_2, \end{cases}$$

where $|u| \leq 1$, with $q_1 = (y_1, z_1)$, $q_2 = (y_2, z_2)$ denote the coordinates of spin 1 and spin 2 and $(1 - \varepsilon)$, $\varepsilon > 0$ small, is the <u>rescaling factor</u> of the control maximal amplitude. Hence, the <u>saturation problem of a pair of spins</u> consists into a simultaneous steering of the couple from $q_1(0) = q_2(0) = N$ to the center $q_1(t_f) = q_2(t_f) = O$, where t_f is the transfer time. The optimal control that we shall analyze is the <u>time minimal saturation</u>, *i.e.* we aim to minimize the transfer time t_f.

2.2. **Maximum principle and singular extremals.**

2.2.1. *Preliminaries.* In this section, we consider a single-input control system: $\frac{\mathrm{d}q}{\mathrm{d}t} = F + u\,G$, where F, G are $\mathcal{C}^\omega$ vector fields defined on an open subset $V \subset \mathbb{R}^n$ and the control u is a bounded measurable mapping defined on $[0, T(u)]$ and valued in $|u| \leq 1$. For fixed q_0 and $T > 0$, the <u>extremity mapping</u> is the map $E \colon u \in L^\infty([0, T]) \mapsto E(u) = q(T, q_0, u)$, where $q(\cdot, q_0, u)$ is the solution of the system with $q(0, q_0, u) = q_0$. A control $u \in L^\infty([0, T])$ is called <u>singular</u> if the extremity mapping is not of full rank and the corresponding trajectory is called singular on $[0, T]$. We have the following relations with the time minimal control problem [31].

Proposition 2.1. *Consider the time minimal control problem for the single-input control system:* $\frac{\mathrm{d}q}{\mathrm{d}t} = F + u\,G$, $|u| \leq 1$. *If $u(\cdot)$, with corresponding trajectory $q(\cdot)$, is solution, then there exists $p(\cdot)$, $t \mapsto p(t) \in \mathbb{R}^n \setminus \{0_{\mathbb{R}^n}\}$, such that the following*

equations are satisfied for the triplet $(q(\cdot), p(\cdot), u(\cdot))$:

(2.3)
$$\dot{q} = \frac{\partial H}{\partial p}, \quad \dot{p} = -\frac{\partial H}{\partial q} \quad a.e.$$

(2.4)
$$H(q(t), p(t), u(t)) = \max_{|v| \leq 1} H(q(t), p(t), v) \quad a.e.$$

Moreover, $M(q, p) = \max_{|v| \leq 1} H(q, p, v)$ is constant along $(q(\cdot), p(\cdot))$ and non-negative, with $H(q, p, u) = p \cdot (F + u\,G)$ the pseudo-Hamiltonian and p is called the adjoint vector.

Definition 2.2. A triplet $(q(\cdot), p(\cdot), u(\cdot))$ solution of (2.3) and (2.4) is called an extremal. It is called regular if $u(t) = \text{sign}(p(t) \cdot G(q(t)))$ *a.e.* and bang-bang if it is regular and the number of switchings of $u(\cdot)$ is finite. An extremal is called singular if $p(\cdot) \cdot G(q(\cdot)) = 0$ everywhere. We denote by σ_+, σ_- and σ_s respectively bang with $u = +1$, $u = -1$ and singular extremals. Extremals satisfying the boundary conditions are called BC-extremals

Proposition 2.3. *If the control $u(\cdot)$ is singular on $[0, T]$ (for the extremity mapping), with $q(\cdot)$ the associated trajectory, then there exists $p(\cdot)$ such that $(q(\cdot), p(\cdot), u(\cdot))$ is a singular extremal.*

2.2.2. *Computation of singular trajectories.* The Lie bracket of two $\mathcal{C}^\omega$ vector fields X, Y on V is computed with the convention:

$$[X, Y](q) = \frac{\partial Y}{\partial q}(q)\, X(q) - \frac{\partial X}{\partial q}(q)\, Y(q),$$

and denoting H_X, H_Y the Hamiltonian lifts: $H_X(z) = p \cdot X(q)$, $H_Y(z) = p \cdot Y(q)$, with $z = (q, p) \in V \times \mathbb{R}^n$, the Poisson bracket reads:

$$\{H_X, H_Y\} = \mathrm{d}H_Y \cdot \overrightarrow{H}_X = p \cdot [X, Y](q),$$

where $\overrightarrow{H}_X = \frac{\partial H}{\partial p}\frac{\partial}{\partial q} - \frac{\partial H}{\partial q}\frac{\partial}{\partial p}$. Differentiating twice $p(\cdot) \cdot G(q(\cdot))$ with respect to the time t, one gets:

Proposition 2.4. *Singular extremals $(z(\cdot), u(\cdot))$ are solutions of the following equations:*

$$H_G(z(t)) = \{H_F, H_G\}(z(t)) = 0,$$

$$\{H_F, \{H_F, H_G\}\}(z(t)) + u(t)\,\{H_G, \{H_F, H_G\}\}(z(t)) = 0.$$

If $\{H_G, \{H_F, H_G\}\} \neq 0$ along the extremal, then the singular control is called of minimal order and it is given by the dynamic feedback:

$$u_s(z(t)) = -\frac{\{H_F, \{H_F, H_G\}\}(z(t))}{\{H_G, \{H_F, H_G\}\}(z(t))}.$$

From the above proposition one gets:

Corollary 2.5. *If $u(\cdot) = 0$ is a singular control on $[0, T]$ then one has:*

$$\mathrm{ad}^k H_F \cdot H_G(z(t)) = p(\cdot) \cdot (\mathrm{ad}^k F \cdot G(q(t))), \quad \forall\, k \geq 0,$$

with $\mathrm{ad}\, F \cdot G = [F, G]$, $\mathrm{ad}\, H_F \cdot H_G = \{H_F, H_G\}$.

The following lemma is useful [5, p. 213].

Lemma 2.6. *For generic pair (F, G) for the Whitney topology, $\dim \text{span}\{\mathrm{ad}^k F \cdot G, \ k \geq 0\} = n$.*

Corollary 2.7. *Up to the time reparameterization*

$$\mathrm{d}s = \frac{\mathrm{d}t}{\{H_G, \{H_F, H_G\}\}(z(t))},$$

singular extremals of minimal order are solutions of the analytic differential equation:

$$\frac{\mathrm{d}z}{\mathrm{d}s} = X(z),$$

with

$$X = \Big(\{H_G, \{H_F, H_G\}\} F - \{H_F, \{H_F, H_G\}\} G\Big)\frac{\partial}{\partial q}$$
$$- \Big(\{H_G, \{H_F, H_G\}\} \frac{\partial F}{\partial q} - \{H_F, \{H_F, H_G\}\} \frac{\partial G}{\partial q}\Big)\frac{\partial}{\partial p},$$

with two constraints $H_F(z) = \{H_F, H_G\}(z) = 0$.

2.2.3. *Classification of singular extremals and time optimality properties.* In this section we recall results of [12] concerning singular extremals. We consider the C^ω-single input control system relaxing the control bound $|u| \leq 1$

$$\dot{q} = F(q) + u\, G(q), \quad u \in \mathbb{R}.$$

Let $\gamma(t) = (q(t), p(t))$, $t \in [0, T]$ be a reference singular extremal of minimal order and we assume that $t \mapsto q(t)$ is one-to-one. Assuming F, G not collinear along $q(\cdot)$ one can assume that $q(\cdot)$ is a singular extremal associated to $u_s \equiv 0$. The first order Pontryagin cone $K(t)$ is the subspace of codimension ≥ 1 generated by the vectors $\mathrm{ad}^k F \cdot G(q(t))$, $k \geq 0$. We introduce the following generic assumptions

  (H1) $\forall t \in [0, T]$, $\mathrm{ad}^2 F \cdot G(q(t)) \notin K(t)$
  (H2) $\forall t$, $K(t)$ is exactly of codimension one and generated by the vectors $\{\mathrm{ad}^k F \cdot G(q(t)); k = 0, \ldots n - 2\}$.
  (H3) If $n \geq 3$, $\forall t \in [0, T]$, $F(q(t)) \in \mathrm{span}\{\mathrm{ad}^k F \cdot G(q(t)); k = 0, \ldots, n - 3\}$.

Under these assumptions, the problem is <u>normal</u> that is the adjoint vector $p(\cdot)$ associated to $q(\cdot)$ is unique up to a factor and $\forall t \in [0, T]$, $p(t)$ is orthogonal to $K(t)$. Orienting $p(\cdot)$ using the convention of the Maximum Principle: $\langle p(t), F(q(t))\rangle \geq 0$, the singular trajectory is called

  - *Hyperbolic* if $\langle p(t), \mathrm{ad}^2(G \cdot F(q(t)))\rangle > 0$.
  - *Elliptic* if $\langle p(t), \mathrm{ad}^2(G \cdot F(q(t)))\rangle < 0$.
  - *Exceptional* if $\langle p(t), X(q(t))\rangle = 0$.

Note that the condition $\langle p(t), \mathrm{ad}^2(G \cdot F(q(t)))\rangle \geq 0$ amounts to the generalized <u>genralized Legendre-Clebsch</u> condition

$$\frac{\partial}{\partial u}\frac{\mathrm{d}^2}{\mathrm{d}t^2}\frac{\partial H}{\partial u}(\gamma(t)) \geq 0$$

and according to the <u>higher-order maximum principle</u> [20], this condition is a necessary (small) time minimization condition. The key result is the following.

Theorem 2.8. *Under assumptions $(H_1), (H_2)$ and (H_3) an exceptional or hyperbolic (respectively elliptic) is time minimizing (respectively time maximizing) on $[0, T]$ with respect to all trajectories contained in a C^0-neighbourhood of $q(\cdot)$ if $T < t_{1c}$ where $t_{1c} > 0$ is called the first conjugate time along $q(\cdot)$.*

Algorithms to compute the fist conjugate times are described in [4] and are implemented in the `HamPath` code.

This gives a complete characterization of the time minimality status of the singular extremals under (generic) assumptions. The control bound $|u| \leq 1$ has been relaxed. In this classification, the control bound $|u_s| \leq 1$, that is the <u>singular arc is admissible</u> to complete the analysis. The case $|u_s| = 1$ corresponds to saturation. If $|u_s| > 1$, the singular control is not admissible and with some abuse, we shall use the terminology <u>parabolic arc</u> for the corresponding trajectory. See [21] for this terminology.

3. Time minimal saturation of a single spin

We refer to [34, 13] for the standard concepts of <u>regular synthesis</u> used in our analysis. We have two cases:

- case 1: fix the initial point to be the North Pole $N = (0, 1)$;
- case 2: fix the final point to be the center $O = (0, 0)$.

We shall only analyze the first case. We complete results from [11] and give new insights.

3.1. **Lie brackets computations.** The system (2.2) is written as:

$$\frac{\mathrm{d}q}{\mathrm{d}t} = F(q) + u \, G(q), \quad |u| \leq 1,$$

with

$$F(q) = -\Gamma \, y \frac{\partial}{\partial y} + \gamma \, (1 - z) \frac{\partial}{\partial z}, \quad G(q) = -z \frac{\partial}{\partial y} + y \frac{\partial}{\partial z},$$

and we can write

$$F(q) = Aq + a, \quad A = \begin{pmatrix} -\Gamma & 0 \\ 0 & -\gamma \end{pmatrix}, \quad a = \begin{pmatrix} 0 \\ \gamma \end{pmatrix}, \quad G(q) = Bq, \quad B = \begin{pmatrix} 0 & -1 \\ 1 & 0 \end{pmatrix}.$$

The system can be lifted on the semi-direct product $\mathrm{GL}(2, \mathbb{R}) \times_s \mathbb{R}^2$ acting on the q-space by the action $(A, a) \cdot q = Aq + a$, and where the Lie bracket rule is: $[(A, a), (B, b)] = ([A, B], Ab - Ba)$, with $[A, B] = AB - BA$ the commutator. One writes

$$A = \mu \, I_2 + \begin{pmatrix} \lambda & 0 \\ 0 & -\lambda \end{pmatrix},$$

with $\mu = -\frac{\Gamma + \gamma}{2}$, which is zero if and only if $\gamma = -\Gamma$ and $\lambda = \frac{\delta}{2}$, where $\delta = \gamma - \Gamma$. The case $\delta = 0$ is the case of <u>water species</u>. Otherwise, we have:

Lemma 3.1. *If $\delta \neq 0$, the Lie algebra generated by (A, a), $(B, 0)$ is $\mathrm{gl}(2, \mathbb{R}) \oplus \mathbb{R}^2$.*

This provides a <u>rough</u> classification of the problems between the simple water case and the general case.

Moreover, all the Lie brackets can be easily computed. They are listed next, up to length 4.
Length 1.

$$F(q) = -\Gamma \, y \frac{\partial}{\partial z} + \gamma \, (1 - z) \frac{\partial}{\partial z}, \quad G(q) = -z \frac{\partial}{\partial y} + y \frac{\partial}{\partial z},$$

Length 2.

$$[F, G](q) = (\delta\, z - \gamma) \frac{\partial}{\partial y} + \delta\, y \frac{\partial}{\partial z}.$$

Length 3.

$$[F, [F, G]](q) = \left(\gamma\, (\gamma - 2\Gamma) - \delta^2\, z\right) \frac{\partial}{\partial y} + \delta^2\, y \frac{\partial}{\partial z},$$

$$[G, [F, G]](q) = 2\, \delta\, y \frac{\partial}{\partial y} + (\gamma - 2\, \delta\, z) \frac{\partial}{\partial z}.$$

Length 4.

$$[F, [F, [F, G]]](q) = (\gamma\, \Gamma\, (\gamma - 2\Gamma) - \gamma\, \delta^2 + \delta^3\, z) \frac{\partial}{\partial y} + \delta^3 y \frac{\partial}{\partial z}$$

$$= \gamma\, \Gamma\, (\gamma - 2\Gamma) \frac{\partial}{\partial y} + \delta^2\, [F, G](q),$$

$$[G, [F, [F, G]]](q) = [F, [G, [F, G]]](q) = -\gamma\, (\gamma - 2\Gamma) \frac{\partial}{\partial z},$$

$$[G, [G, [F, G]]](q) = (\gamma - 4\, \delta\, z) \frac{\partial}{\partial y} - 4\, \delta\, y \frac{\partial}{\partial z} = -3\, \gamma \frac{\partial}{\partial y} - 4\, [F, G](q).$$

3.2. **Frame curves, collinearity and singular loci.** The collinearity locus $\mathscr{C}$ is defined as the set where F and G are linearly dependent and the singular set $\mathscr{S}$ is where F and $[F, G]$ are collinear. Computing, one has:

Lemma 3.2. *The collinearity set $\mathscr{C}$ is given by $\gamma z(1 - z) - \Gamma y^2 = 0$, thus O and N belong to $\mathscr{C}$. Under the assumption $0 < \gamma \leq 2\Gamma$, $\mathscr{C}$ is an ellipse contained in the Bloch ball. Besides, for each point q of $\mathscr{C}$, except O, there exists u such that q is an equilibrium point of the dynamics $F + u\, G$.*

The dynamics reads $F(q) + u\, G(q) = Mq + a$, $M = A + u\, B$, so for the maximal amplitude $u = +1$, the corresponding equilibrium point is

$$O_1 = -M^{-1} a = \frac{\gamma}{u^2 + \gamma\, \Gamma} \begin{pmatrix} -u \\ \Gamma \end{pmatrix} = \frac{\gamma}{1 + \gamma\, \Gamma} \begin{pmatrix} -1 \\ \Gamma \end{pmatrix} \in \mathscr{C}$$

and it is contained in the sector $y < 0$. We define in the same way O_{-1} for $u = -1$.

Lemma 3.3. *The singular trajectories are located on $\mathscr{S}$ which is given by $y(\gamma - 2\delta z) = 0$. Hence, it is the union of the z-axis of revolution $y = 0$ and the horizontal line $z = \gamma/(2\delta)$, providing $\delta \neq 0$. Under the assumption $0 < \gamma \leq 2\Gamma$, $\mathscr{S}$ intersects the Bloch ball if and only if $3\gamma \leq 2\Gamma$. In this case, $z_s = \gamma/(2\delta) \in [-1, 0)$.*

The singular control is given by solving

$$D'(q) + u\, D(q) = 0,$$

with $D = \det(G, [G, [F, G]])$ and $D' = \det(G, [F, [F, G]])$. For $y = 0$, $D(q) = -z(\gamma - 2\delta z)$ and $D' = 0$. Hence, the singular control is zero and the singular trajectories are solution of $\dot{y} = -\Gamma y = 0$, $\dot{z} = \gamma(1 - z)$. The North Pole is an equilibrium which is a stable node for $0 < \gamma \leq 2\Gamma$. Along the horizontal singular line, *i.e.* for $z = \gamma/2\delta$, one has $D(q) = -2\delta y^2$, $D'(q) = \gamma y(2\Gamma - \gamma)$ and the singular control denoted u_s is given by $u_s(q) = \gamma(2\Gamma - \gamma)/(2\delta y)$. Hence, along the singular horizontal direction, the singular flow is: $\dot{y} = -\Gamma y - \gamma^2(2\Gamma - \gamma)/(4\delta^2 y)$, $\dot{z} = 0$, and one has $u_s \to \pm\infty$ when $y \to 0^{\mp}$.

Main assumptions. Under the physical assumptions

$$0 < \gamma \leq 2\Gamma,$$

the Bloch ball is invariant for the dynamics. Besides, under the physical assumption and

$$|\delta| < 2,$$

any positive bang arc solution of $\dot{q} = F(q) + G(q) = Mq + a$ spirals around O_1 and converges to it (O_1 is a stable spiral), since in this case M has two complex conjugate eigenvalues with negative real part. Likewise, negative bang arcs spirals around O_{-1}.

Proposition 3.4. *If $\gamma > 0$ and $|\delta| < 2$, then the solution of $\dot{q} = F(q) + G(q)$, $q(0) = q_0$ is given by:*
(3.1)

$$q(t) = \exp((\alpha - \gamma)t) \begin{pmatrix} \frac{\alpha}{\beta}\sin(\beta t) + \cos(\beta t) & -\frac{1}{\beta}\sin(\beta t) \\ \frac{1}{\beta}\sin(\beta t) & -\frac{\alpha}{\beta}\sin(\beta t) + \cos(\beta t) \end{pmatrix} (q_0 - O_1) + O_1,$$

where $\alpha = \delta/2$ and $\beta = \sqrt{1 - \alpha^2}$. The solution is quasi-periodic of period $T = 2\pi/\beta$.

Proposition 3.5. *Let $(y(\cdot), z(\cdot))$, with associated control $u(\cdot)$, be a trajectory solution of (2.2). Then, $(-y(\cdot), z(\cdot))$ with control $-u(\cdot)$ is also solution of (2.2).*

This discrete symmetry allows us to consider only trajectories in the domain $y \leq 0$ of the Bloch ball.

Notation. We denote by S_1 the intersection of the positive bang arc σ_+ issued from the North Pole with the horizontal singular line $z = z_s = \gamma/2\delta$, and by S_1' the intersection with the vertical singular line $y = 0$. S_1 and S_1' may not exist for specific values of (γ, Γ). We denote by S_3 the point on the horizontal singular line such that σ_+ is tangent to this line at this point, *i.e.* S_3 is a saturation point for the singular control u_s ($u_s(S_3) = 1$), and by S_3' the intersection of the bang arc σ_+ issued from S_3 with the axis $y = 0$. If $0 < \gamma \leq 2\Gamma$ is satisfied, then S_3 is in the domain $y < 0$ if $\delta < 0$. We define in the same way S_{-3} for $u = -1$. See Fig. 1 to visualize on an example: the singular and collinearity sets, the points S_1, S_1', S_3, S_3'...

3.3. **Switching function, the concept of bridge and the θ function.**

3.3.1. *Switching function.* Let $z(t)$, $t \in [0, T]$, be an extremal curve. The <u>switching function</u> is defined as $\Phi(t) = p(t) \cdot G(q(t))$. A time t is called an <u>ordinary switching time</u> if $\Phi(t) = 0$ and $\dot{\Phi}(t) \neq 0$, *i.e.* $p(t) \cdot G(q(t)) = 0$ and $p(t) \cdot [F, G](q(t)) \neq 0$. In the 2D-case, outside the collinearity set, one can write:

$$[F, G](q) = \alpha(q) F(q) + \beta(q) G(q),$$

with

$$\alpha(q) = \frac{\det(G(q), [F, G](q))}{\det(G(q), F(q))}.$$

At an ordinary switching time t, one has:

$$\text{sign}(\dot{\Phi}(t)) = \text{sign}(\alpha(q(t))),$$

with the convention of the maximum principle, *i.e.* $H_F \geq 0$. If $\alpha(q(t)) > 0$, then we switch from an arc σ_- to an arc σ_+ and the converse if $\alpha(q(t)) < 0$. Fig. 2 gives the sign of α inside the Bloch ball for fixed parameters γ and Γ.
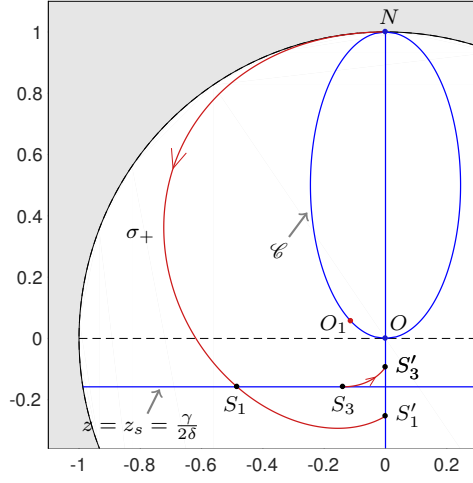
FIGURE 1. Collinearity set, singular set and visualization of N, O, O_1, S_1, S_1', S_3 and S_3'. In this example, $(\gamma, \Gamma) = (0.12, 0.5)$.
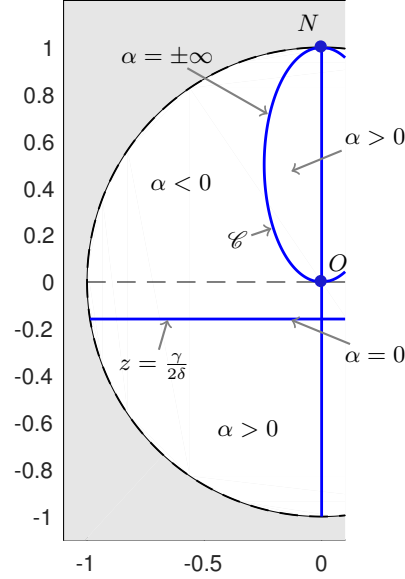

FIGURE 2. Sign of $\alpha(q)$ in the domain $y \leq 0$. The sign in the domain $y \geq 0$ is given by symmetry. In this example, $(\gamma, \Gamma) = (0.12, 0.5)$.

3.3.2. *The concept of Bridge.* An arc σ_+ or σ_- corresponding to $u = +1$ or $u = -1$, is called a <u>bridge</u> on $[0, t]$ if the extremities correspond to non ordinary switching points, *i.e.* $\Phi(0) = \dot{\Phi}(0) = \Phi(t) = \dot{\Phi}(t) = 0$, see Fig. 3.

Remark 3.6. This concept is important and leads to a generalization in higher dimension, which plays an important role in the time minimal saturation of a pair of spins, but also in the contrast problem.
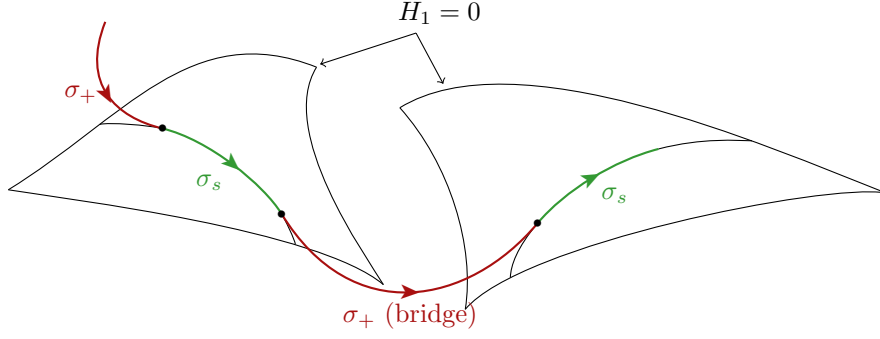
FIGURE 3. An extremal of the form $\sigma_+\sigma_s\sigma_+\sigma_s$ is portrayed in the cotangent space, where σ_+ and σ_s represent respectively bang and singular extremals. The second bang arc is a bridge.
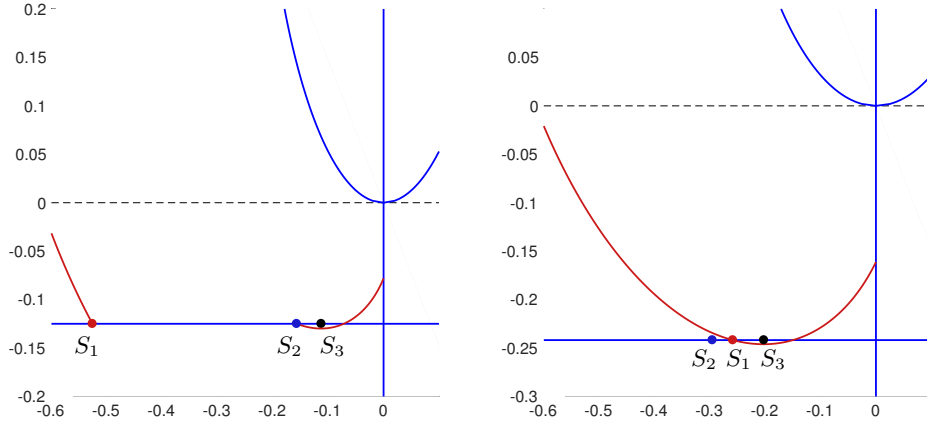

FIGURE 4. The points S_1, S_2 and S_3 with different orders. On the left sub-graph: $(\gamma, \Gamma) = (0.1, 0.5)$ and on the right: $(\gamma, \Gamma) = (0.163, 0.5)$.

If a bridge σ_+, in the domain $y \leq 0$, connecting the horizontal and vertical singular lines exists, then we denote by S_2 the extremity on $z = \gamma/2\delta$, and S_2' the other extremity on $y = 0$. We observe two cases when S_2 exists which are crucial for the analysis of the time minimal saturation problem of a single spin, see Fig. 4.

3.3.3. *Analysis of two consecutive switching times.* In the 2D-case, in order to analyze switchings, one proceeds as follows. Assume 0 and t be two consecutive switching times on an arc σ_+ or σ_-. Let $z(\cdot) = (q(\cdot), p(\cdot))$ denote the associated extremal. We have:

$$p(0) \cdot G(q(0)) = p(t) \cdot G(q(t)) = 0.$$

We denote by $v(\cdot)$ the solution on $[0, t]$ of the variational equation

$$\dot{v}(t) = \left(\frac{\partial F}{\partial q}(q(t)) + u \frac{\partial G}{\partial q}(q(t)) \right) v(t), \quad v(t) = G(q(t)), \quad u = \pm 1.$$

This equation is integrated backwards from time t to 0. By construction, $p(\cdot) \cdot v(\cdot)$ is constant and equal to zero. At time 0, one has $p(0) \cdot v(0) = p(0) \cdot G(q(0)) = 0$. Hence, $p(0)$ is orthogonal to $v(0)$ and to $G(q(0))$. Therefore, $v(0)$ and $G(q(0))$ are collinear ($p(\cdot)$ does not vanish, according to proposition 2.1). We introduce naturally the $\theta(t)$ function which gives the angle between $G(q(0))$ and $v(0)$ measured counterclockwise. One deduces that switchings occur at times 0 and t if

$$\theta(t) = 0 \mod \pi$$

and it can be tested using $\det(G(q(0)), v(0)) = 0$. This test may be used by contraposition in order to eliminate the possibility that bang-bang trajectories with at least two switching times (or more) are optimal. We have by definition

$$v(0) = e^{-t \operatorname{ad}(F + u\,G)}(G(q(t)), \quad u = \pm 1,$$

and in the analytic case, the ad-formula gives:

$$v(0) = \sum_{n \geq 0} \frac{(t)^n}{n!} \operatorname{ad}^n(F + u\,G) \cdot G(q(t)).$$

The computation can be made explicit on a Lie group since determining $\exp(t \operatorname{ad}(F + u\,G))$ amounts to compute a Jordan form of the linear operator $\operatorname{ad}(F + u\,G)$ defined by the Lie brackets.

3.4. Optimality status.
A first step in the optimality analysis is to discriminate between small time minimizing or maximizing singular trajectories using the high-order maximum principle and Theorem 2.8. In dimension 2, we introduce $D'' = \det(G, F)$ and $D'' = 0$ is the collinearity set $\mathscr{C}$. Singular lines are fast if $D\,D'' > 0$ and slow if $D\,D'' < 0$. Using these conditions, if $0 < \gamma$ and $\delta < 0$, then the horizontal singular line $z = z_s$ is fast if $y \neq 0$. For the interesting case when the horizontal singular line cuts the Bloch ball, *i.e.* when $0 < 3\gamma \leq 2\Gamma$, the singular horizontal line is fast. Moreover, it is parabolic on $(S_3\,, S_{-3}) = \{(1 - \lambda)S_3 + \lambda S_{-3} \mid \lambda \in (0\,, 1)\}$ when $y \neq 0$ and hyperbolic otherwise (except of course at S_3 and S_{-3}). On the other hand, assuming $0 < \gamma \leq 2\Gamma$ and considering only the interesting part inside the Bloch ball, then we have the following: if $\delta < 0$, then the vertical line is hyperbolic for $z_s < z < 1$ and elliptic for $-1 \leq z < z_s$. If $\delta > 0$, then it is hyperbolic for $-1 \leq z < 1$.

Theorem 2.8 combined with the generalized Legendre-Clebsch condition gives information about the local optimality of the singular extremals. In the 2D-case, global optimality can be analyzed using the clock form $\omega = p \cdot \mathrm{d}q$ with $p \cdot G = 0$ and $p \cdot F = 1$. The clock form may be used to compare two trajectories with the same extremities whenever they do not cross the collinearity set. In the time minimal saturation problem of a single spin, the collinearity set plays a crucial role and we must use the θ function defined in section 3.3 to eliminate the possibility to have two consecutive ordinary switching times.

To complete the study, we have to analyze the behavior of optimal trajectories in the neighborhood of some particular points, named Frame Points corresponding to isolated singularities: intersection of the collinearity locus with singular locus or singular loci [13]. In the time minimal saturation problem, there exists two phenomena to analyze. The horizontal singular line being admissible up to a saturation

point S_3, there is a birth of a switching locus Σ_3[1] connecting the horizontal and vertical singular lines. This is related to the concept of bridge and this phenomenon is referred as the SiSi singularity [11]. The time minimal synthesis, with initial point N, is represented on Figs. 9, 10 and 11. The interaction between the collinearity and singular sets near the North Pole is the second phenomenon to analyze and is refered as the SiCo singularity[11]. Near the North Pole, only bang-bang trajectories with at most one switching are optimal (see the top part of Fig. 9).

According to the sections 3.5, 3.6, 3.7 and 3.8 and according to the Figs. 9, 10 and 11, we have the following results.

Theorem 3.7. *Let us denote by σ_+^N the positive bang arc starting from the North Pole with S_1, S_1' respectively the intersection points (they may not exist) with the horizontal, vertical singular line. Let us denote by σ_+^b the bridge with S_2 and S_2' as extremities, by σ_s^h, σ_s^v respectively a horizontal, vertical singular arc. Let S_3 denote the saturation point on the horizontal singular line and S_3' the intersection of the bang arc starting from S_3 with the axis $y = 0$.*

For parameters (Γ, γ) satisfying the physical constraints $0 < \gamma \leq 2\Gamma$, and such that the points S_1' and S_3' are below the origin O, then the minimal time trajectory to steer the spin from N to O is $NS_1S_2S_2'O$, i.e. it is of the form $\sigma_+^N\sigma_s^h\sigma_+^b\sigma_s^v$ (no empty arcs), if σ_+^N intersects the horizontal singular line strictly before S_2, that is $S_1 < S_2$. Otherwise, the optimal trajectory is $NS_1'O$, i.e. of the form $\sigma_+^N\sigma_s^v$.

3.5. **Parameters and practical cases.** The optimal syntheses depend on the parameters (γ, Γ). We define in this section the domain of interest of the parameters and partition it in four main sub-domains which are denoted A_1, A_2, B and C. This partitioning may be visualized on Fig. 5.

We have already seen that we assume $0 < \gamma \leq 2\Gamma$ and $|\delta| < 2$, with $\delta = \gamma - \Gamma$. Additionally, we require that the origin O is accessible from the North Pole N, that is we impose that S_1' is below O. The parameters such that $S_1' = O$ are given by the following proposition:

Proposition 3.8. *For $\gamma > 0$, we have:*

$$S_1' = O \iff \exp\left((t_0\,\beta + \pi)\,\frac{\alpha - \gamma}{\beta}\right) - \gamma = 0,$$

with

$$t_0 = \begin{cases} \frac{1}{\beta}\arctan\left(-\frac{\beta}{\alpha}\right) & \text{if} \quad \delta < 0, \\ \frac{\pi}{2} & \text{if} \quad \delta = 0, \\ \frac{1}{\beta}\left(\arctan\left(-\frac{\beta}{\alpha}\right) + \pi\right) & \text{if} \quad \delta > 0. \end{cases}$$

Besides, to simplify the presentation, we restrict the analysis to the case where S_3' is below O. This implies that the origin may be reached from the horizontal singular locus going through the bridge. We have the following relation on the parameters to impose $S_3' = O$:

Proposition 3.9.

$$S_3' = O \iff (2\Gamma^2 - \gamma\Gamma + 1)\exp\left((\alpha - \gamma)t_0\right) - 2|\delta| = 0.$$

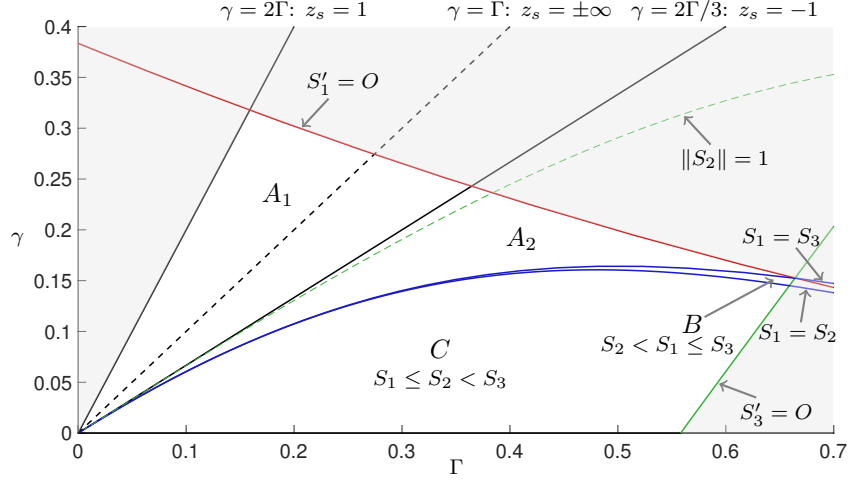[1]We denote by Σ the switching locus with strata Σ_1, Σ_2...

FIGURE 5. The domain of interest of the parameters in white with the sub-domains A_1, A_2, B and C.

One can notice according to Fig. 5 that if $0 < \gamma \leq 2\Gamma$ is satisfied and if the points S_1' and S_3' are below the origin O, then $|\delta| < 2$ holds. We restrict the analysis of the optimal syntheses to these values of parameters. Let us explain now how we partition this domain. We denote by A_1 the sub-domain such that $2\Gamma/3 \leq \gamma \leq 2\Gamma$ and S_1' is below O. In this case, S_1' is necessarily below O, the horizontal singular line (at $z = z_s = \gamma/2\delta$) does not cut the interior of the Bloch ball and the optimal synthesis is simple, see section 3.8. Now, when the horizontal singular line cuts the interior of the Bloch ball, that is for $0 < \gamma < 2\Gamma/3$, this part of the singular locus does not play any role if the bang arc starting from the North Pole does not intersect it, that is if S_1 does not exist. The limit case is when $S_1 = S_3$, where S_3 is the saturation point on the horizontal singular line. We denote by A_2 this sub-domain of parameters and we have the same optimal syntheses in A_1 and A_2, see again section 3.8.

Proposition 3.10.

$$S_1 = S_3 \iff (2\Gamma^2 - \gamma\Gamma + 1)\frac{\gamma}{2\delta} + \exp\left((\alpha - \gamma)\frac{\pi}{\beta}\right) = 0.$$

The remaining part, when S_1 exists, may be split in two. Either, S_1 is before S_2 (S_2 is one of the extremities of the bridge) or after. We denote by B the sub-domain where $S_2 < S_1$ (*i.e.* S_2 strictly before S_1) and C where $S_1 \leq S_2$. One can visualize the sub-domains A_1, A_2, B and C on the Fig. 5.

Remark 3.11. Each specie to study is characterized by its relaxation times T_1 and T_2, see Table 1. However, the main parameter is the ratio T_2/T_1. According to Fig. 6, one can see that for any couple (T_1, T_2) such that $0 < T_2 < 2T_1/3$, then there exists $\omega_{max} > 0$ such that the associated parameters (γ, Γ), see eq. (2.1), belongs to the sub-domain C. Hence, for any couple (T_1, T_2) satisfying the physical constraint $0 < T_2 \leq 2T_1$, there exists $\omega_{max} > 0$ such that the associated parameters (γ, Γ) belongs either to A_1 or C.
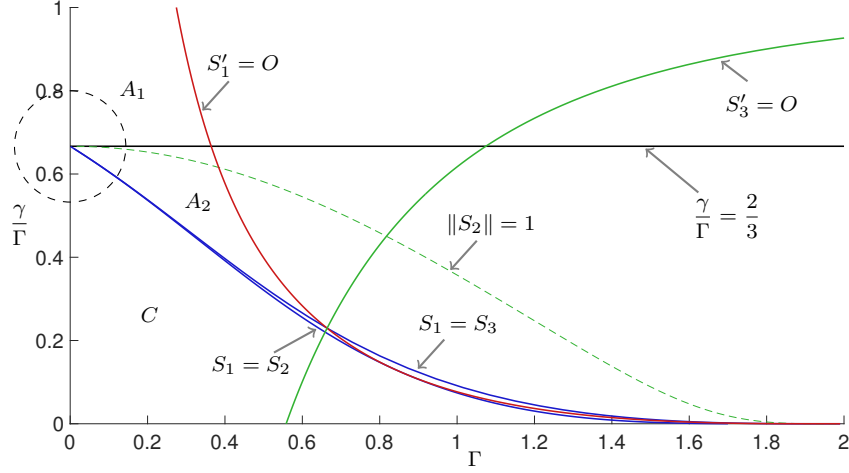
FIGURE 6. The sub-domains in $(\Gamma, \gamma/\Gamma)$ coordinates. One can notice that when Γ tends to 0, then the slopes of the curves $S_1 = S_2$ and $S_1 = S_3$, in (Γ, γ) coordinates, are equal to 2/3.
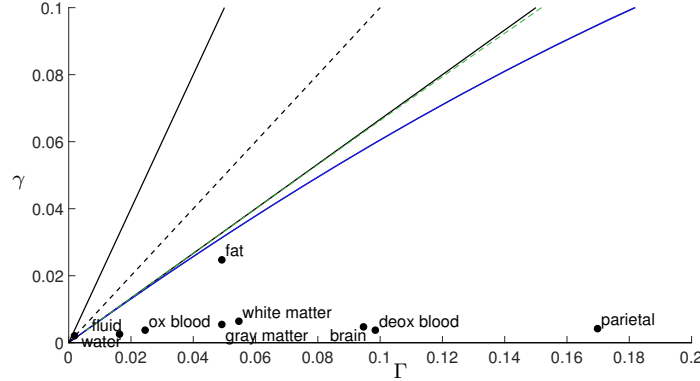

FIGURE 7. The associated (γ, Γ) parameters of cases from Table 1 with $\omega_{\max} = 2\pi \times 32.3$ Hz. Except the water case which is in the sub-domain A_1, all the others cases belong to the sub-domain C.

In Fig. 7, we show for the practical cases from Table 1, the associated (γ, Γ) parameters with $\omega_{\max} = 2\pi \times 32.3$ Hz. Note that in the experiments, $\omega_{\max}$ may be chosen up to 15 000 Hz but we consider here the same value as in [11]. The water case belongs to the domain A_1 while all the others cases are contained in C. In Fig. 8 is represented the slope $T_2/T_1 = \gamma/\Gamma$ with the particular case when $\omega_{\max} = 2\pi \times 32.3$ Hz. One can notice that the fat case is the only one which crosses the sub-domains A_2, B and C but for the value $\omega_{\max} = 2\pi \times 32.3$ Hz, it belongs to C.

3.6. **The optimal synthesis in the sub-domain** C. For the optimal synthesis in the sub-domain C, we have the following: the parameters satisfy $0 < 3\gamma < 2\Gamma$, the point S_3' is below the origin O and there exist S_1 and S_2 such that $S_1 \leq S_2 < S_3$, *i.e.* we are in the situation of the left sub-graph of Fig. 4. In this case, the horizontal singular line cuts the Bloch ball in the domain $-1 < z < 0$ and the global synthesis
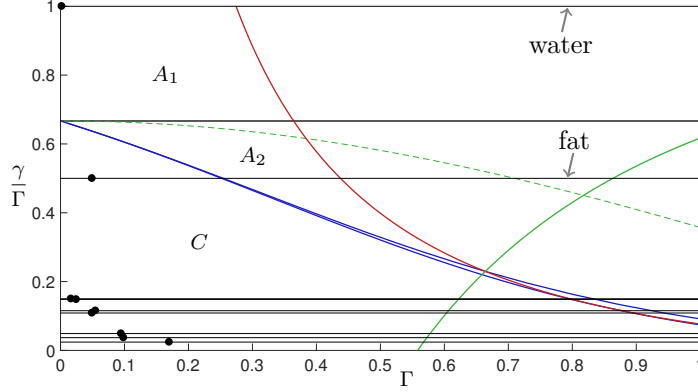
FIGURE 8. The slopes $T_2/T_1 = \gamma/\Gamma$ for the species from Table 1 with the particular case when $\omega_{\max} = 2\pi \times 32.3$ Hz. This particular case is represented by a bullet while the slope is represented by a line. One can notice that the fat case is the only one which can belong to the domains A_2, B and C. The water case belongs only to A_1 while the others belong only to C.

is similar as the one presented in [11]. It is obtained gluing together the SiSi and SiCo cases and it is represented on the Fig. 9.

Remark 3.12. In [11], to obtain this optimal synthesis, it is assumed that $\omega_{\max}$ is large enough. Remark 3.11 explains why this assumption is correct. However, this assumption is replaced here by geometric relations on the points S_1, S_2 and S_3'.

The switching locus is formed by the positive bang arc starting from the North Pole (denoted σ_+^N) and reaching the horizontal singular arc at S_1 (it is denoted Σ_1 in the figure), by the horizontal singular segment Σ_2 between the points S_1 and S_3, the switching locus Σ_3 due to the saturation phenomenon and by the part of the vertical singular direction between S_2' and O (the Σ_4 segment), S_2' being the extremity of the bridge on $y = 0$. The bang arc with $u = -1$ starting from S_1 splits the domain in two sub-domains, one with a bang-bang policy and the other containing a non trivial singular arc.

We have, as a corollary, that in this case, the optimal strategy to steer the system from the North Pole to the origin in minimum time is of the form $\sigma_+^N \sigma_s^h \sigma_+^b \sigma_s^v$, where σ_s^h and σ_s^v denote respectively horizontal and vertical singular arcs, and where σ_+^b is the bridge.

Remark 3.13. Note that the switching locus has a complex structure, but due to the symmetry, all the cut points, i.e. the first points where the extremal trajectories cease to be optimal, are on the vertical z-axis where two symmetric solutions starting respectively on the left and right part of the Bloch ball intersect at the same time.

3.7. **The optimal synthesis in the sub-domains B.** For the optimal synthesis in the sub-domain B, we have the following: the parameters satisfy $0 < 3\gamma < 2\Gamma$, the point S_3' is below the origin O and there exist S_1 and S_2 such that $S_2 < S_1 \leq S_3$, *i.e.* we are in the situation of the right sub-graph of Fig. 4. In this case, the horizontal singular line cuts the Bloch ball in the domain $-1 < z < 0$ and still plays a role.
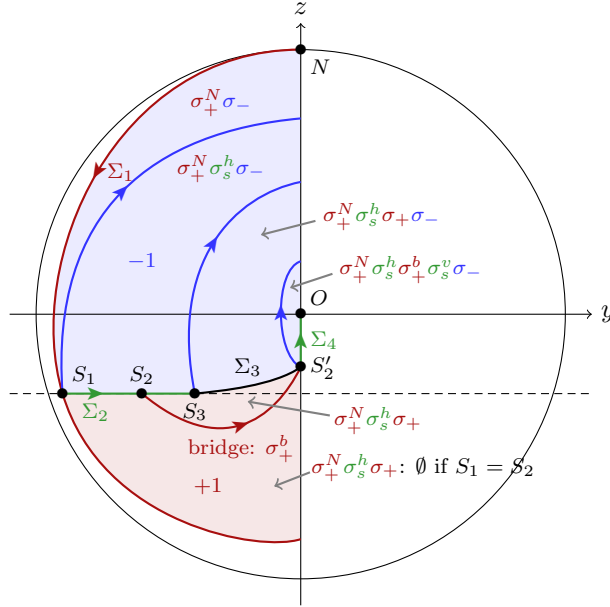
FIGURE 9. Schematic time minimal synthesis to steer a single spin system from the North Pole N to any point of the Bloch ball in the reachable set, for parameters $(\Gamma, \gamma) \in C$. An arbitrary zoom has been used to construct the figure. The set of Σ_i forms the switching surface Σ dividing the $+1$ and -1 areas respectively in red and blue. The minimal time trajectory to steer the spin from N to O is $NS_1S_2S_2'O$, $i.e.$ it is of the form $\sigma_+^N \sigma_s^h \sigma_+^b \sigma_s^v$ with horizontal σ_s^h and vertical σ_s^v singular arcs. The spin leaves the horizontal singular arc before the point S_3 (where the control saturates the constraint) producing a bridge σ_+^b to reach the vertical singular line.

The switching locus is formed by the positive bang arc starting from the North Pole (denoted σ_+^N) and reaching the horizontal singular arc at S_1 (denoted Σ_1), by the horizontal singular segment Σ_2 between the points S_1 and S_3, by the switching locus Σ_3 due to the saturation phenomenon from S_3 to the intersection with σ_+^N (denoted S_1''), by the part of σ_+^N between S_1'' and S_1' (denoted Σ_5) and by the part of the vertical singular direction between S_1' and O (the Σ_4 segment), S_1' being the extremity of σ_+^N on $y = 0$.

We have, as a corollary, that in this case, the optimal strategy to steer the system from the North Pole to the origin in minimum time is of the form $\sigma_+^N \sigma_s^v$.

Remark 3.14. Note that the switching locus is located on the vertical z-axis due to the symmetry.

3.8. **The optimal synthesis in the sub-domains A_1 and A_2.** For the optimal synthesis in the sub-domains A_1 and A_2, we have the following: the parameters satisfy $0 < \gamma \leq 2\Gamma$, the point S_1' is below the origin O and σ_+^N does not intersect the horizontal singular line $z = z_s = \gamma/2\delta$, that is S_1 does not exist. In this case, the horizontal singular line does not play any role.
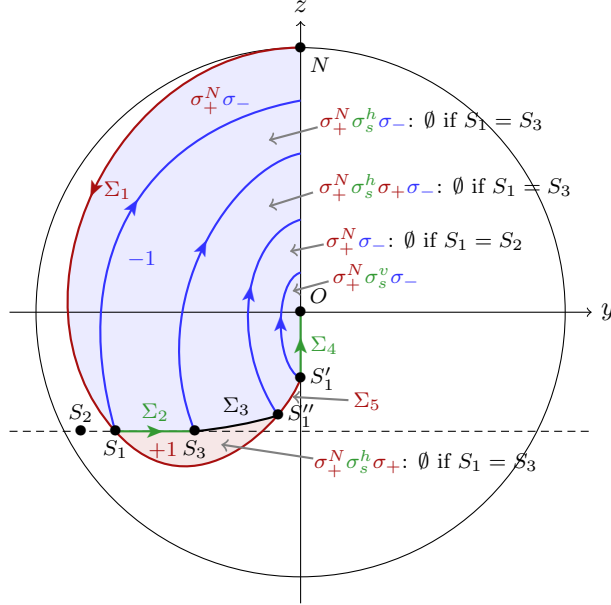
FIGURE 10. Schematic time minimal synthesis to steer a single
spin system from the North Pole N to any point of the Bloch ball
in the reachable set, for parameters $(\Gamma, \gamma) \in B$. An arbitrary zoom
has been used to construct the figure. The set of Σ_i forms the
switching surface Σ dividing the $+1$ and -1 areas respectively in
red and blue. The minimal time trajectory to steer the spin from
N to O is $NS_1'O$, *i.e.* it is of the form $\sigma_+^N \sigma_s^v$.

The switching locus is formed by the positive bang arc starting from the North
Pole (denoted σ_+^N) and reaching the vertical singular arc at S_1' (denoted Σ_1) and
by the part of the vertical singular direction between S_1' and O (the Σ_4 segment).

We have, as a corollary, that in this case, the optimal strategy to steer the system
from the North Pole to the origin in minimum time is of the form $\sigma_+^N \sigma_s^v$ as in the
sub-domain B.

Remark 3.15. Note that the switching locus is located on the vertical z-axis due to
the symmetry.

3.9. Geometric comments and construction of a normal form.

Lie brackets computations. At the intersection q_{0s} of the horizontal and vertical
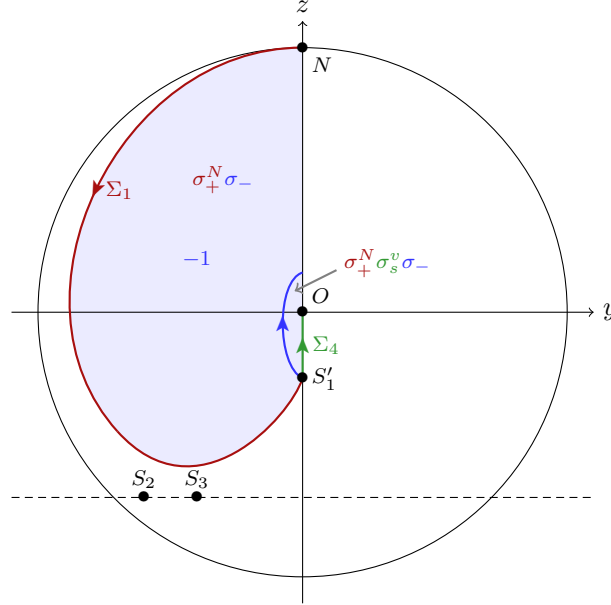lines the Lie algebraic structure up to order four is described by:

FIGURE 11. Schematic time minimal synthesis to steer a single spin system from the North Pole N to any point of the Bloch ball in the reachable set, for parameters $(\Gamma, \gamma) \in A_2$. For $(\Gamma, \gamma) \in A_1$, the synthesis is the same but there is no horizontal singular line inside the Bloch ball. An arbitrary zoom has been used to construct the figure. The minimal time trajectory to steer the spin from N to O is NS'_1O, $i.e.$ it is of the form $\sigma^N_+ \sigma^v_s$.

$$F(q_{0s}) = \gamma \left(1 - \gamma/(2\,\delta)\right)\frac{\partial}{\partial z}, \quad G(q_{0s}) = -\gamma/(2\,\delta)\,\frac{\partial}{\partial y},$$

$$[F,G](q_{0s}) = -\gamma/2\,\frac{\partial}{\partial y},$$

$$[F,[F,G]](q_{0s}) = (\gamma\,(\gamma - 2\Gamma) - \delta\,\gamma/2)\,\frac{\partial}{\partial y},$$

$$[G,[F,G]](q_{0s}) = 0,$$

$$[F,[F,[F,G]]](q_{0s}) = \gamma\,\Gamma\,(\gamma - 2\Gamma - \delta^2\,\gamma/2)\frac{\partial}{\partial y},$$

$$[G,[F,[F,G]]](q_{0s}) = -\gamma\,(\gamma - 2\Gamma)\frac{\partial}{\partial z},$$

$$[G,[G,[F,G]]](q_{0s}) = -\gamma\frac{\partial}{\partial y}.$$

This led to the algebraic characterization of some specific bridges, related to this case.

Normal form. A normal form to make an explicit evaluation of the synthesis in the neighbourhood of zero of size ε is obtained by choosing parameters in such a way that the points S_2 and S_3 are contained in this neighbourhood.

Limit syntheses. Since the singular control u_s is L^1 when $q \to q_{0s}$ stay on the horizontal singular line, one has:

Proposition 3.16. *Relaxing $|u| \leq 1$, we have two limit time minimal solutions to steer N to O*

- $2\Gamma > 3\gamma > 0 : R\,\sigma_s^h\,\sigma_s^v$,
- $2\Gamma \leq 3\gamma : R\,\sigma_s^v$,

where R is the rotation with respect to the center O to reach either the horizontal singular line or the vertical singular line.

4. TIME MINIMAL SATURATION OF A PAIR OF SPIN-1/2 PARTICLES

4.1. **The model.** Let us consider a couple of spins with the same characteristics, *i.e.* the same relaxation times T_1 and T_2, but for which for each, the control field has different intensities, because of inhomogeneities. The system we consider is the following:

$$(4.1) \quad \begin{aligned} \dot{q}_1(t) &= F(q_1(t)) + u(t)\,G(q_1(t)), \\ \dot{q}_2(t) &= F(q_2(t)) + u(t)\,(1-\varepsilon)\,G(q_2(t)), \end{aligned}$$

where $q_i = (y_i, z_i)$, $i = 1, 2$, denote the coordinates of each system and where the vector fields F and G are given by eq. (2.2), see sections 2.1 and 3.1. The term $(1-\varepsilon)$, $\varepsilon > 0$ small, is the rescaling factor of the control maximal amplitude. We define the <u>time minimal saturation problem of a pair of spin-1/2 particles</u> as the following affine control problem with Mayer cost:

$$(P_{BS}) \quad \begin{cases} J(u(\cdot), t_f) = t_f \longrightarrow \min \\ \dot{q}(t) = F(q(t)) + u(t)\,G(q(t)), \quad |u(t)| \leq 1, \quad t \in [0, t_f], \quad q(0) = q_0, \\ q(t_f) = q_f, \end{cases}$$

where $q = (q_1, q_2) = (y_1, z_1, y_2, z_2)$, $q_0 = (0, 1, 0, 1)$, $q_f = (0, 0, 0, 0)$, and where we use the notation

$$F(q) = F(q_1)\frac{\partial}{\partial q_1} + F(q_2)\frac{\partial}{\partial q_2},$$

$$G(q) = G(q_1)\frac{\partial}{\partial q_1} + (1-\varepsilon)\,G(q_2)\frac{\partial}{\partial q_2}.$$

We have the following Lie brackets up to order 3:

$$[F, G](q) = [F, G](q_1)\frac{\partial}{\partial q_1} + (1-\varepsilon)\,[F, G](q_2)\frac{\partial}{\partial q_2},$$

$$[F, [F, G]](q) = [F, [F, G]](q_1)\frac{\partial}{\partial q_1} + (1-\varepsilon)\,[F, [F, G]](q_2)\frac{\partial}{\partial q_2},$$

$$[G, [F, G]](q) = [G, [F, G]](q_1)\frac{\partial}{\partial q_1} + (1-\varepsilon)^2\,[G, [F, G]](q_2)\frac{\partial}{\partial q_2}.$$

4.2. **Some prior theoretical results.** We present some theoretical results in relation with numerical homotopies. They are based on Lie brackets computations.

Lemma 4.1. span$\{\mathrm{ad}^k F \cdot G; \ k \geq 0\} = \mathrm{span}\{\mathrm{ad}^k F \cdot G; \ k = 0, 1, 2, 3\}$.

Proposition 4.2. *For all q in the Bloch ball, for all pair of parameters (Γ, γ), we have* $\det(G(q), [F, G](q), [F, [F, G]](q), [F, [F, [F, G]]](q)) = 0$ *and every solution of $F(q)$ is a (smooth) singular trajectory.*

Lemma 4.3. *In the water case $\gamma = \Gamma$, $\mathrm{ad}^2 F \cdot G$ is constant and collinear to $[F, G]$.*

Proposition 4.4. *In the water case $\gamma = \Gamma$, the only singular trajectories are the (smooth) solutions of $F(q)$.*

Next, we present some accessibility criteria.

Lemma 4.5. *A necessary condition to steer the North pole $(0, 1, 0, 1)$ to $(0, 0, 0, 0)$ is that for the second spin the arc σ_+ starting from $(0, 1)$ reaches the vertical axis $y_2 = 0$ at a point $(0, z)$, $z \leq 0$.*

Definition 4.6. The center O is called η-reachable if there exists O' of the collinearity locus such that $|O - O'| \leq \eta$ and O' is a point of the collinear locus such $(F + u_0 G)(O') = O$ and O' is globally stable.

4.3. **First numerical results and validation with LMI methods.**

4.3.1. *Direct approach (`Bocop`).* The `Bocop` software [3] implements a so-called direct transcription approach, where the continuous optimal control problem (OCP) is transformed into a nonlinear programming (NLP). The reformulation is done by a discretization of the time interval, with an approximation of the dynamics of the system by a generalized Runge-Kutta scheme. This is part of direct local collocation methods. We refer the reader to for instance [2], [18] and [30] for more details on direct transcription methods and NLP algorithms.

We present local solutions obtained by the `Bocop` software for the bi-saturation problem ($\mathrm{P_{BS}}$) in the Desoxygenated blood case (denoted C_1), the Oxygenated blood case (C_2) and the Cerebrospinal fluid case (C_3) with $\omega_{\max} = 2\pi \times 32.3$ and the Water case (C_4) with a larger value of $\omega_{\max}$. Let us mention that for C_4, the value of $\omega_{\max}$ is larger than $2\pi \times 32.3$ just to obtain a control law with longer bang arcs, to visualize better the solution. The parameter ε is fixed to 0.1 and let us recall that the associated relaxation times are given in Table 1. The time evolution of the state variables $q = (q_1, q_2)$ and of the control variable u are represented in Figs. 12–15, the optimal time is given in Table 2 and is compared with the optimal time for the saturation of the single spin. Note that for each case, there is one more Bang-Singular sequence (the first one) in the bi-saturation problem than in the mono-saturation problem. Besides, the remaining part looks like the strategy to steer one single spin to the center of the Bloch ball except that for C_1, C_2 and C_3, the penultimate singular part of the trajectory do not follow exactly the horizontal lines $z_1 = z_2 = z_s = \gamma/2\delta$, $\delta = \gamma - \Gamma$. Finally, note that both spins reach the vertical line $y_1 = y_2 = 0$ with $z_1 = z_2$ before the final singular arc with $u = 0$ to reach the center of the Bloch ball at the same time. In other words, the spins are synchronised at this time.

Case	Γ	γ	t_f (2 spins)	t_f (1 spin)
C_1	9.855×10^{-2}	3.65×10^{-3}	44.769	42.685
C_2	2.464×10^{-2}	3.65×10^{-3}	113.86	110.44
C_3	1.642×10^{-2}	2.464×10^{-3}	168.32	164.46
C_4	9.855×10^{-2}	9.855×10^{-2}	15.0237	8.7445

TABLE 2. Cases treated numerically corresponding respectively to the Desoxygenated case (C_1), the Oxygenated case (C_2), the Cerebrospinal fluid case (C_3) and the Water case (C_4). The 5th (resp. 4th) column gives the final time found by `Bocop` for the saturation of one spin (resp. two spins with B_1-inhomogeneity). The parameter ε is fixed to 0.1.
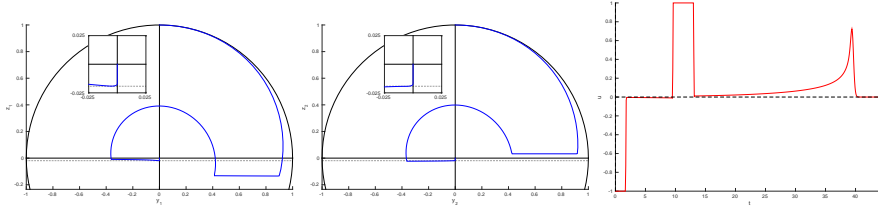

FIGURE 12. Desoxygenated blood case (C_1) with RF-inhomogeneity ($\varepsilon = 0.1$). Trajectories for spin 1 and 2 in the (y,z)-plane are portrayed in the first two subgraphs. The corresponding control is drawn in the right subgraph. The horizontal lines $z_1 = z_2 = z_s = \gamma/2\delta$, $\delta = \gamma - \Gamma$, is represented by dashed lines. Note that the last bang arc is not well captured by the direct solver because it is too short.
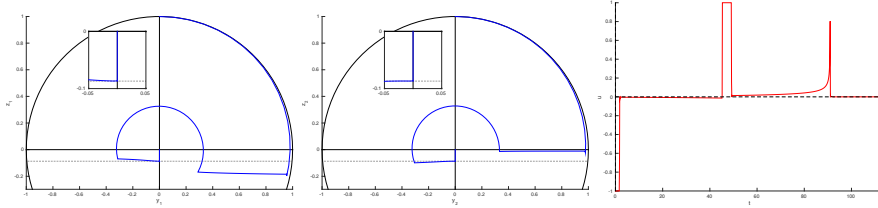

FIGURE 13. Oxygenated blood case (C_2) with RF-inhomogeneity ($\varepsilon = 0.1$). Trajectories for spin 1 and 2 in the (y,z)-plane are portrayed in the first two subgraphs. The corresponding control is drawn in the right subgraph. The horizontal lines $z_1 = z_2 = z_s = \gamma/2\delta$, $\delta = \gamma - \Gamma$, is represented by dashed lines. Note that the last bang arc is not well captured by the direct solver because it is too short.

4.3.2. *LMI method (`GloptiPoly`).* A crucial step is to check whether the local optimal times presented in Table 2 and obtained with `Bocop` for the saturation problem are globally optimal using moment/LMI techniques. More precisely, these techniques provide for the saturation problem, lower bounds on the global optimal
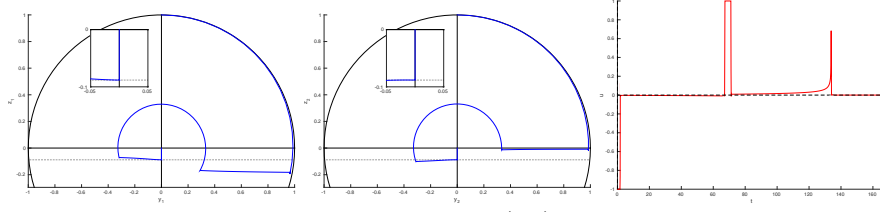
FIGURE 14. Cerebrospinal fluid case (C_3) with RF-inhomogeneity $(\varepsilon = 0.1)$. Trajectories for spin 1 and 2 in the (y,z)-plane are portrayed in the first two subgraphs. The corresponding control is drawn in the right subgraph. The horizontal lines $z_1 = z_2 = z_s = \gamma/2\delta$, $\delta = \gamma - \Gamma$, is represented by dashed lines. Note that the last bang arc is not well captured by the direct solver because it is too short.
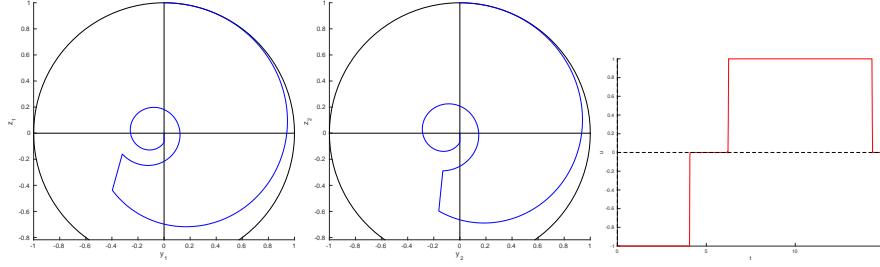

FIGURE 15. Water case (C_4) with RF-inhomogeneity $(\varepsilon = 0.1)$. Trajectories for spin 1 and 2 in the (y,z)-plane are portrayed in the first two subgraphs.

time which can be used as a validation of the global optimality if the gap between the lower bound obtained from moment/LMI techniques and the time obtained by the direct method is small. This combination of techniques has already been successful in the contrast problem [8] by nuclear magnetic resonance in medical imaging.

The moment approach is a global optimization method which relaxes a non linear optimal control problem using measures as a linear programming (LP) problem. In the case where the data are polynomials, we can handle these measures by their moment sequences. Using powerful certificate coming from algebraic geometry, *e.g. Putinar's Positivstellensatz* [32], this leads to an infinite dimensional LMI problem which can be truncated to a finite set of moments. The sequence of optimal values associated to these truncated problems converges to the optimal value of problem ($\mathrm{P_{BS}}$), that we denote by $T^*_{\min}$. We present a classical formulation and an alternative one which exploits the structure of the problem, based on [16]. Note that we present the method on the bi-saturation problem but it is straightforward to adapt the explanations for the mono-saturation problem.

Notations. B_n is the unit ball of dimension n, $\mathcal{M}^+(Z)$ is the set of finite, positive Borel measures supported on compact set Z and $\int f(z)\,d\mu$ denotes the integration of a continuous function $f \in C(Z)$ with respect to $\mu \in \mathcal{M}^+(Z)$.

Step 1: linear program on measures.

- **1st formulation: Moment approach using occupation measures.**

  Following [25], the problem $(\mathrm{P_{BS}})$ can be embed into the linear program on measures:

  $$T_{LP} = \inf_{\mu,\mu_f} \int \mathrm{d}\mu_f$$
  $$\text{s.t.} \int \left(\frac{\partial v}{\partial t} + \frac{\partial v}{\partial q}\,(F + u\,G) \right) \mathrm{d}\mu \tag{4.2}$$
  $$= \int v(\cdot, q_f)\,\mathrm{d}\mu_f - v(q_0), \quad \forall v \in \mathbb{R}[t,q],$$
  $$\mu \in \mathcal{M}^+([0,T] \times Q \times U), \quad \mu_f \in \mathcal{M}^+(Q_f),$$

  and where T is fixed, $Q_f = [0,T] \times \{(0,0,0,0)\}$, $Q = B_2 \times B_2$ are admissible state sets and $U = B_1$ is the admissible control set. Given any admissible pair $(q(\cdot), u(\cdot))$ for $(\mathrm{P_{BS}})$, it corresponds a measure μ admissible for (4.2) achieving the same cost, hence $T^*_{\min} \geq T_{LP}$. Moreover, according to Theorem 3.6 (ii) of [25], there is no optimality gap and

  $$T^*_{\min} = T_{LP}.$$

  Remark 4.7. Since the dynamic is autonomous, the time variable can be removed and the LP problem becomes

  $$T_{LP} = \inf_{\mu} \int \mathrm{d}\mu$$
  $$\text{s.t.} \int \frac{\partial v}{\partial q}\,(F + uG)\,\mathrm{d}\mu = v(q_f) - v(q_0), \quad \forall v \in \mathbb{R}[q], \tag{4.3}$$
  $$\mu \in \mathcal{M}^+(Q \times U).$$

- **2nd formulation: Moment approach using modal occupation measures.**

  In the first formulation (4.2) (respectively (4.3)), measures are supported on the set $[0,T] \times Q \times U$ (respectively $Q \times U$) of dimension $1 + 4 + 1 = 6$ (respectively 5) and we expect them to be located on the optimal trajectory $(q^*(\cdot), u^*(\cdot))$. An alternative formulation [16] is to model controls by measures such that the measures are supported on Q only. Indeed, note that the dynamic in $(\mathrm{P_{BS}})$ is affine in the control u which takes its values inside the polytope $\mathrm{conv}\{-1, +1\}$. This optimal control problem can be written as a switching system with two modes, the first mode corresponding to $u = +1$ and the second mode corresponding to $u = -1$. This leads to consider

  $$T_{LP'} = \inf_{\mu_1,\mu_2,\mu_f} \int \mathrm{d}\mu_f$$
  $$\text{s.t.} \quad \forall v \in \mathbb{R}[t,q], \int \left(\frac{\partial v}{\partial t} + \frac{\partial v}{\partial q}\,(F + G) \right) \mathrm{d}\mu_1 \tag{4.4}$$
  $$+ \int \left(\frac{\partial v}{\partial t} + \frac{\partial v}{\partial q}\,(F - G) \right) \mathrm{d}\mu_2 = \int v(\cdot, q_f)\,\mathrm{d}\mu_f - v(0, q_0),$$
  $$\mu_1, \mu_2 \in \mathcal{M}^+([0,T] \times Q), \quad \mu_f \in \mathcal{M}^+(Q_f)$$

where T is fixed, $Q_f = [0, T] \times \{(0, 0, 0, 0)\}$ and $Q = B_2 \times B_2$ are admissible state sets.

Step 2: Moment SDP. An important feature of the problems (4.2)-(4.4) is their algebraic structure: the dynamic is polynomial and the sets Q and U are compact basic semi-algebraic sets. In these settings, it is possible to handle the measures by their moments which leads to a semi-definite program on countably many moments. Let us introduce for a multi-index $\alpha = (\alpha_1, \dots, \alpha_p) \in \mathbb{N}^p$ and $y = (y_1, \dots, y_p) \in \mathbb{R}^p$, the notation $|\alpha|_1 = \sum_{i=1}^p \alpha_i$ and y^α which stands for the monomial $y_1^{\alpha_1} \dots y_p^{\alpha_p}$. Then, we denote by $\mathbb{N}_d^p$ the set $\{\alpha \in \mathbb{N}^p \mid |\alpha|_1 \le d\}$.

Definition 4.8. The moment of order $\alpha \in \mathbb{N}^p$ of a measure μ supported on $Z \subset \mathbb{R}^p$ is the real $y_\alpha = \int z^\alpha \, d\mu$. Besides, $\mu \in \mathcal{M}(z)$ is said to be a representing measure for a sequence $(y_\alpha)_\alpha$ if $y_\alpha = \int z^\alpha \, d\mu$ for all $\alpha \in \mathbb{N}^p$.

Definition 4.9. Given an arbitrary sequence of reals $(y_\alpha)_\alpha$, we define the Riesz linear functional $l_y \colon \mathbb{R}[z] \to \mathbb{R}$ by $l_y(z^\alpha) = y_\alpha$ for all $\alpha \in \mathbb{N}^p$.

Definition 4.10. The moment matrix $M_d(y)$ of order d is such that $l_y(p(z)^2) = p' M_d(y) p$ for all polynomials $p(z)$ of degree d whose coefficients are denoted by the vector p. In particular, the (i, j)th entry is $M_d(y)[i, j] = l_y(z^{i+j}) = y_{i+j}$, $\forall i, j \in \mathbb{N}_d^p$.

Similarly, the localizing matrix of order d associated with a sequence (y_α) and a polynomial $g(z)$ is the matrix $M_d(g\,y)$ such that $l_y(g(z)\,p(z)^2) = p' M_d(g\,y) p$ for all polynomial $p(z)$ of degree d.

Proposition 4.11. *Let Z be a compact basic semi-algebraic set defined by $Z = \{z \in \mathbb{R}^p \mid g_k(z) \ge 0, \ k = 1, \dots, n_Z\}$. Then, a necessary condition for a sequence $(y_\alpha)_\alpha$ to have a representing measure $\mu \in \mathcal{M}^+(z)$ is*

$$M_d(y) \succeq 0, \quad M_d(g_k\,y) \succeq 0, \quad \forall d \in \mathbb{N}, \forall k = 1, \dots, n_Z.$$

Finally, we introduce

$$[0, T] \times Q \times U = \{(t, q, u) \mid q = (q_{11}, q_{12}, q_{21}, q_{22}), \ g_1(t, q, u) := t(T - t) \ge 0,$$
$$g_2(t, q, u) := 1 - q_{11}^2 - q_{12}^2 \ge 0, \ g_3(t, q, u) := 1 - q_{21}^2 - q_{22}^2 \ge 0,$$
$$g_4(t, q, u) := 1 - u^2 \ge 0\},$$

and

$$Q_f = \{(t, q) \in \mathbb{R}^5 \mid g_0^f(t) := t(T - t) \ge 0, \ g_1^f(q) := q_{11} = 0,$$
$$g_2^f(q) := q_{12} = 0, \ g_3^f(q) := q_{21} = 0, \ g_4^f(q) := q_{22} = 0\}.$$

We denote by l_{y^μ}, $l_{y^{\mu_f}}$ the Riesz functionals associated respectively with the sequences y^μ and y^{μ_f}. Then, the moment SDP problem associated with (4.2) is

$$T_{SDP} = \inf_{y^\mu, y^{\mu_f}} l_{y^{\mu_f}}(1)$$

$$l_{y^\mu}\left(\frac{\partial v}{\partial t} + \frac{\partial v}{\partial q}(F + uG)\right) = l_{y^{\mu_f}}(v(\cdot, q_f)) - v(0, q_0), \quad \forall v \in \mathbb{R}[t, q], \quad (4.5)$$
$$M_d(y^\mu) \succeq 0, \ M_d(g_i\,y^\mu) \succeq 0, \ i = 1 \dots 4, \ \forall d \in \mathbb{N},$$
$$M_d(y^{\mu_f}) \succeq 0, \ M_d(g_i^f\,y^{\mu_f}) \succeq 0, \ i = 0 \dots 4, \ \forall d \in \mathbb{N}.$$

At the end, according to Proposition 4.11, we have $T_{LP} \ge T_{SDP}$ and this is in fact an equality according to Theorem 3.8 from [24].

Step 3: Hierarchy of SDP problems. Note that $M_{d+1}(y) \succeq 0$ implies $M_d(y) \succeq 0$. The LMI constraints and the sequence (y_α) of (4.5) are truncated which lead to $r \geq 1$ to the Lasserre's hierarchy parameterized by $r \geq 1$

$$T_{LMI}^r = \inf_{(y_\alpha^\mu)_{|\alpha| \leq 2r}, (y_\alpha^{\mu_f})_{|\alpha| \leq 2r}} l_{y^{\mu_f}}(1)$$

$$l_{y^\mu}\left(\frac{\partial v}{\partial t} + \frac{\partial v}{\partial q}(F + uG)\right) = l_{y^{\mu_f}}(v(\cdot, q_f)) - v(0, q_0), \quad \forall v \in \mathbb{R}[t, q], \quad (4.6)$$

$$M_r(y^\mu) \succeq 0, \ M_{r-s_i}(g_i \, y^\mu) \succeq 0, \ i = 1 \dots 4$$

$$M_r(y^{\mu_f}) \succeq 0, \ M_r(g_i^f \, y^{\mu_f}) \succeq 0, \ i = 0 \dots 4.$$

where $s_i = \deg(g_i)/2$ if $\deg(g_i)$ is even and $s_i = (\deg(g_i) + 1)/2$ otherwise. The main result is then the following.

Proposition 4.12 (Theorem 5.6, [24]). *We have*

$$T_{\min}^* = T_{LP} = T_{SDP} \geq \dots \geq T_{LMI}^{r+1} \geq T_{LMI}^r \geq \dots \geq T_{LMI}^1.$$

Moreover the sequence of lower bounds $(T_{LMI}^r)_r$ converges to $T_{\min}^*$ as $r \to \infty$.

Summary of the LMI method. The moment/LMI method approach for optimization consist in reformulating an optimization problem as a linear program on measures. When the data is polynomial, a hierarchy of lmi relaxations can be constructed, whose costs converge to that of the original problem. The strong feature of the method is that those LMI generate lower bounds on the true cost, and can therefore be used as certificates of global optimality. On the other hand, the weak points of the method are its poor algorithm complexity for unstructured problem, as well as for the special case of optimal control, the unavailability of a generic method to recover controls. Note that the passage to a given LMI relaxation starting from measure problem (4.2) or (4.4) can be fully automated with high-level commands using the `GloptiPoly` toolbox [19].

4.3.3. *Validation of the numerical results.* The problem (4.6) corresponds to the multisaturation problem of two spins associated with the LP problem (4.2). Likewise, we can construct from the LP problem (4.4) a hierarchy of LMI relaxations parameterized by r in the single spin case and the two spins case to compare the two formulations. We use the `Mosek` toolbox [29] to solve the SDP problems. Let t_f denote the best solution found with the `Bocop` software, given in Table 2 for the single spin case and the two spins case. The value of the parameters for (4.6) are: $\varepsilon = 0.1$, $q_0 = (0, 1, 0, 1)$, $q_f = (0, 0, 0, 0)$ and $T = t_f$. The lower bounds of T_{min}^* are T_{LMI}^r (resp. $T_{LMI'}^r$) associated with the LP problem (4.2) (resp. (4.4)) and are given in Table 3.

We denote by $n = \dim Q$, $m = \dim U$ and $n_d = 2$ is the number of modes for the second formulation. At the relaxation order d, the number of moments involved in the SDP problem associated with (4.2) and (4.4) is given by $N_m = \binom{n+m+1+2d}{n+m+1} + \binom{n+1+2d}{n+1}$ and $N_m = (n_d + 1)\binom{n+1+2d}{n+1}$ respectively. In Fig. 16 are represented the relative error $\mathrm{err}(r) = (t_f - T_{LMI}^r)/t_f$ for the cases C_1, C_2, C_3 and C_4, where T_{LMI}^r is the optimal value of (4.6) in the single spin case and the two spins case. Note that in the single spin case, we know the structure and the optimal value of the global solution and we can compute the numerical gap between the direct approach and the moment/LMI approach.

Both formulations are computationally demanding, the relative errors on the final

	1st Formulation		2nd Formulation	
r	N_m	$(t_f - T^r_{LMI})/t_f$	N_m	$(t_f - T^r_{LMI'})/t_f$
1	25	0.8143	30	0.818
2	105	0.5164	105	0.5958
3	294	0.2611	252	0.4355
4	660	0.1491	495	0.1842
5	1287	0.0932	858	0.1284
6	2275	0.0643	1365	0.096
7	3740	0.0517	2040	0.0797
8	5814	0.0461	2907	0.0716

TABLE 3. Single spin saturation for the case C_2. T^r_{LMI} is the optimal value of the hierarchy (4.6). Likewise, $T^r_{LMI'}$ is the optimal value of the hierarchy of SDP problems derived from (4.4). $t_f = 110.44$ is the best time found by the `Bocop` software. The second and fourth columns are the relative errors between best solution found by the `Bocop` software and the one found by moment/LMI techniques for each relaxation order r.

times found by `Bocop` for the cases C_2, C_3, C_4 are less than 5% for the single spin saturation and less than 10% for the multisaturation. Note that these two formulations have to be compared not only on the sharpness of the lower bounds but also considering the number of moments involved in the hierarchy.
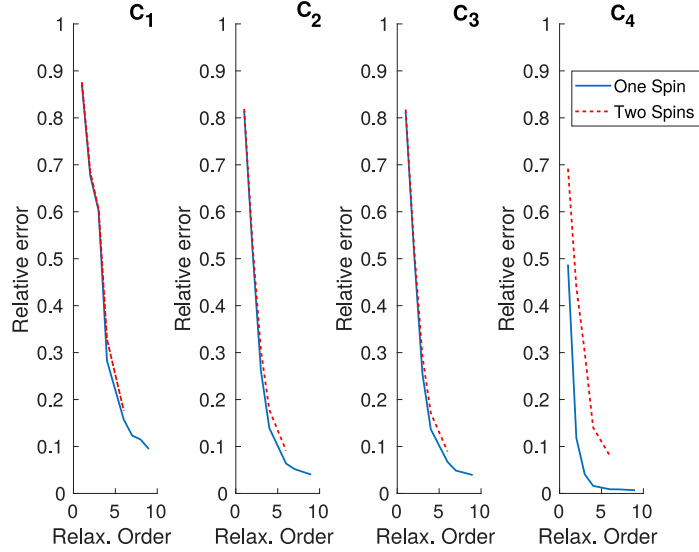

FIGURE 16. Saturation problem of one spin and two spins for the cases C_1, C_2, C_3 and C_4. Relative error $\text{err}(r) = (t_f - T^r_{LMI'})/t_f$ where r is the order of relaxation, $T^r_{LMI'}$ is the optimal value of (4.6) using the formulation (4.4) and t_f is the final time computed with `Bocop`.

4.4. **Influence of the parameters on the BC-extremals.** We use a combination of multiple shooting and differential path following methods to analyze the influence of the parameters on BC-extremals from problem (P_{BS}). We recall the multiple shooting technique in section 4.4.1, we give some details about homotopy and monitoring in section 4.4.2 and we present the results in section 4.4.3.

4.4.1. *Multiple shooting (HamPath).* Since the optimal structures are composed of sequences of bang and singular arcs, we must use multiple shooting instead of single shooting. We refer to [14, 28] for details about multiple shooting algorithms and to [8] and [9] for explanations about multiple shooting in the context of medical imaging. One particularity is that the solutions end with a singular arc and not a bang arc, contrary to the examples given in [28]. Because of that, the shooting equations are more intricate as we can see it hereinafter.

Let $u_s(x, p)$ denote the singular control and $u_\pm = \pm u_{\max} = \pm 1$ the positive and negative bang controls. Let us assume we have a solution with a structure of the form BSBS, *i.e.* Bang-Singular-Bang-Singular. We note $y = (p_0, t_f, t_1, t_2, t_3, z^1, z^2, z^3)$ the unknowns of the shooting function which is given by :

$$
S: \ \mathbb{R}^{32} \quad \longrightarrow \quad \mathbb{R}^{32}
$$

$$
y = \begin{bmatrix} p_0 \\ t_f \\ t_1 \\ t_2 \\ t_3 \\ z^1 \\ z^2 \\ z^3 \end{bmatrix} \longmapsto S(y) = \begin{bmatrix} u_\pm H_1(z^0) + p^0 \\ H_1(z^1) \\ H_{01}(z^1) \\ H_1(z^3) \\ H_{01}(z^3) \\ y_2(t_f, t_3, z^3, u_s) \\ z_2(t_f, t_3, z^3, u_s) \\ (p_{z_1}(t_f, t_3, z^3, u_s) + p_{z_2}(t_f, t_3, z^3, u_s))\gamma + p^0 \\ z(t_1, 0, z^0, u_\pm) - z^1 \\ z(t_2, t_1, z^1, u_s) - z^2 \\ z(t_3, t_2, z^2, u_\pm) - z^3 \end{bmatrix}
$$

where $p^0 = -1$ in the normal case, where $z^0 = (q_0, p_0)$ is the initial state-costate vector with $q_0 = (0, 1, 0, 1)$. To get a BC-extremal we want to solve the shooting equations

$$
S(y) = 0.
$$

The first equation comes from the fact that the final time is free, the four following equations means that the associated extremal becomes singular at z^1 and z^3. The last three matching equations improve numerical stability. Note that we have only three equations (the three remaining equations) associated to the final condition: $q(t_f) = (0, 0, 0, 0)$. This is because we can find a redundant equation and this is due to the fact that the trajectory ends with a singular (and not bang) arc. Indeed, the fact that $H_1(z^3) = H_{01}(z^3) = 0$ implies that $H_1(z(t_f, t_3, z^3, u_s)) =$

$H_{01}(z(t_f, t_3, z^3, u_s)) = 0$. But, if $(p_{y_1}(t_f, t_3, z^3, u_s), p_{z_1}(t_f, t_3, z^3, u_s)) \neq 0$, then

$$\left.\begin{array}{r} H_1(z(t_f, t_3, z^3, u_s)) = 0 \\ H_{01}(z(t_f, t_3, z^3, u_s)) = 0 \\ y_2(t_f, t_3, z^3, u_s) = 0 \\ z_2(t_f, t_3, z^3, u_s) = 0 \\ (p_{z_1}(t_f, t_3, z^3, u_s) + p_{z_2}(t_f, t_3, z^3, u_s))\gamma + p^0 = 0 \end{array}\right\} \Rightarrow \begin{array}{l} y_1(t_f, t_3, z^3, u_s) = \\ z_1(t_f, t_3, z^3, u_s) = 0. \end{array}$$

Hence, for any zero of the shooting function, the associated trajectory reaches the target $q_f = (0, 0, 0, 0)$ at the final time if $(p_{y_1}(t_f, t_3, z^3, u_s), p_{z_1}(t_f, t_3, z^3, u_s)) \neq 0$. Let us recall that one difficulty to solve a shooting equation is to have a good initial guess. To determine the structure and make the shooting method converge, we use direct methods from the `Bocop` software. This combination of direct and indirect methods has already been successful in the contrast problem [8] by nuclear magnetic resonance in medical imaging.

4.4.2. *Homotopy and monitoring.* Once we have a solution obtained by a multiple shooting method, we can use differential homotopy techniques [1] to study the deformation of the solution with respect to the relaxation parameters. The homotopy method, from `HamPath` software [15], is based on Predictor-Corrector algorithm with a high order and step-size control Runge-Kutta scheme for the prediction and with a classical simplified Newton method for the correction. We combine the differential path following method with monitoring at each accepted step of the integration to detect if structural changes occur during the homotopy. We consider three different monitoring for which we give the associated action for the saturation problem:

- check if each arc (except the first and the last arcs) has positive length, that is if $t_i \leq t_{i+1}$. If not, the arc with negative length has to be removed.
- check if the singular control on each singular arc (except the last arc because it is 0) is admissible. If not, one bang arc has to be added.
- check if the switching function on each bang arc remains of constant sign. If not, one singular arc has to be added.

Let us illustrate the third monitoring on an example. We write $\Gamma = \rho \cos \theta$ and $\gamma = \rho \sin \theta$, and we consider an homotopy (called H1a) on θ with $\rho = \bar{\rho} \approx 0.0551$, from $\theta = \theta_{\max} = \text{atan}(2) \approx 1.1071$ to $\theta = \theta_{\min} = 0.02$. One starts from $\theta = \theta_{\max}$ with a structure of the form BSBS ($\sigma_- \sigma_s \sigma_+ \sigma_0$). Around $\theta = \theta_{1a,1} \approx 0.5069$, the monitoring detects a change in the structure. Let us denote by $\theta_{1a,1}^+ \geq \theta_{1a,1} \geq \theta_{1a,1}^-$ the two values of θ at the two consecutive steps such that these inequalities are satisfied. Since, for $\theta = \theta_{1a,1}^-$, the switching function crosses 0 two times on the first bang arc, one has to stop the homotopy and add a singular arc, see figure 17.

4.4.3. *Numerical results.* We write $\Gamma = \rho \cos \theta$ and $\gamma = \rho \sin \theta$, and we consider only homotopies on θ with $\rho = \bar{\rho} \approx 0.0551$. This particular value of ρ is such that we retrieve the fat case, that is $T_1 = 0.2$ and $T_2 = 0.1$, with $u_{\max} = 1$ and $\omega_{\max} = 2\pi \times 32.3$, this specific value of $\omega_{\max}$ being excerpted from [11]. We present some results for a range of values of θ to illustrate the role of this parameter on the structure of some BC-extremals from problem P_{BS}. The value of θ ranges between $\theta = \theta_{\max} = \text{atan}(2) \approx 1.1071$ and $\theta = \theta_{\min} = 0.02$. The maximal bound is chosen to satisfy the physical constraint $0 < \gamma \leq 2\Gamma$ while the minimal bound is chosen
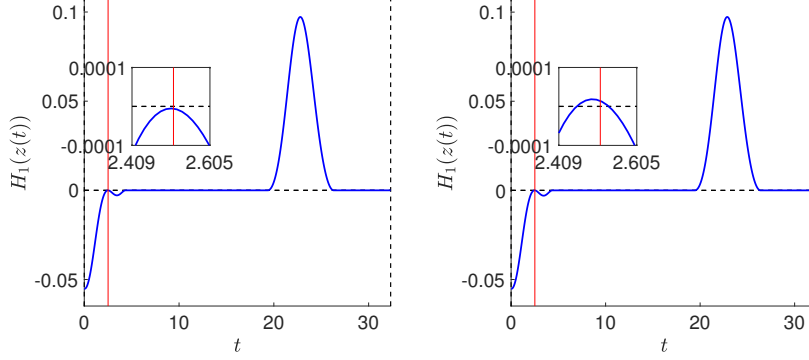
FIGURE 17. Fat case: $\rho = \rho_{\text{fat}}$, $\theta = \theta_{1a,1}^{+}$ (Left) and $\theta = \theta_{1a,1}^{-}$ (Right). Each subgraph represents the graph of the switching function H_1 along the extremal. For $\theta = \theta_{1a,1}^{-}$, we observe that H_1 crosses 0 twice. A singular arc must be added to continue the homotopy on θ. A zoom in on the graph of H_1 is given and may be located thanks to the vertical red lines. Note that we add a singular arc, since in this case the singular extremal is time-minimizing for small time.

to include all the practical cases, see Table 1. The saturation of a pair of spins is a much more complex problem than the mono-saturation, so we do not intend to get any optimal synthesis but just optimal trajectories to steer both spins from the North Pole to the center of the Bloch ball in minimum time and in a synchronized fashion. Besides, we just analyze the influence of θ for fixed values of $\rho = \bar{\rho}$ and $\varepsilon = 0.1$.

The methodology is the following. For a given initial value of θ, we use direct method to determine the structure and to initialize the multiple shooting method. Then, we perform homotopies on θ with monitoring to stop it if necessary. If a change in the structure is detected, then, we update the multiple shooting function and continue the homotopy until we reach the final value of θ if possible. Note that in the multi-saturation problem, there exist many local solutions. Thus, for a given value of θ we must compare the cost of each solution. This leads to compute several path of zeros and then compare them in terms of cost. We choose to present four different paths, see Table 4 and Fig 21. Note that the paths of zeros are computed with a very good accuracy according to the bottom-right subgraph of Fig 21. Before we give some details about the homotopies, we present three particular cases excerpted from these homotopies: the Water case ($\omega_{\max} = 10.2684$), the Fat case ($\omega_{\max} = 202.9469 \approx 2\pi \times 32.3$) and the Cerebrospinal Fluid case ($\omega_{\max} = 61.1840$). See Table 1 for the corresponding values of θ. All the others cases have the same optimal structure than the Cerebrospinal Fluid case. One can see from Fig 21 that for the Water case, the optimal structure is of the form $\sigma_- \sigma_s \sigma_+ \sigma_0$ and the solution is given by the homotopie (H1a). The solution is given on Fig. 18. For the Fat case, the structure is of the form $\sigma_- \sigma_s \sigma_- \sigma_s \sigma_+ \sigma_0$ and it is also given by (H1a), see Fig. 19. Finally, for the Cerebrospinal Fluid case, the structure is of the form $\sigma_- \sigma_s \sigma_+ \sigma_s \sigma_+ \sigma_0$ and it is given by (H1b), see Fig. 20. One can notice different interactions between bang and singular arcs depending on the

case, and one can see that the horizontal line $z = z_s = \gamma/2\delta$ plays a crucial role in the optimal trajectory when it intersects the Bloch ball.
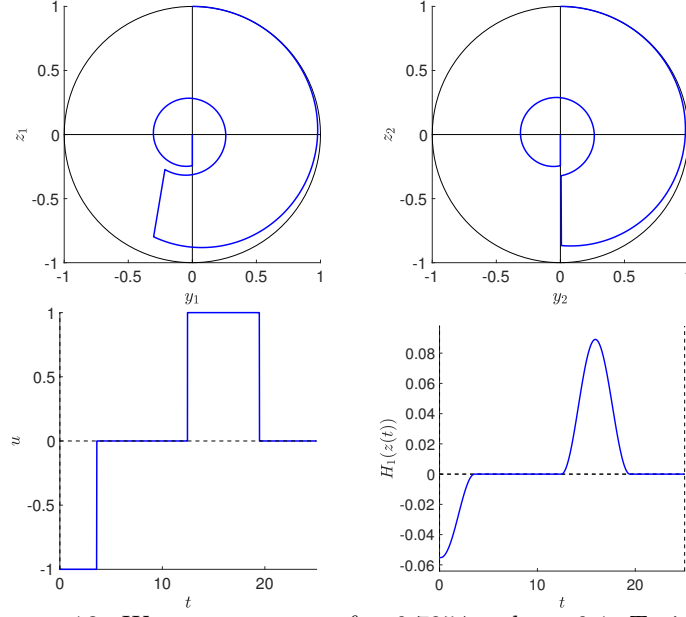

FIGURE 18. Water case: $\rho = \bar{\rho}$, $\theta = 0.7854$ and $\varepsilon = 0.1$. Trajectories of spins 1 and 2, control and H_1.
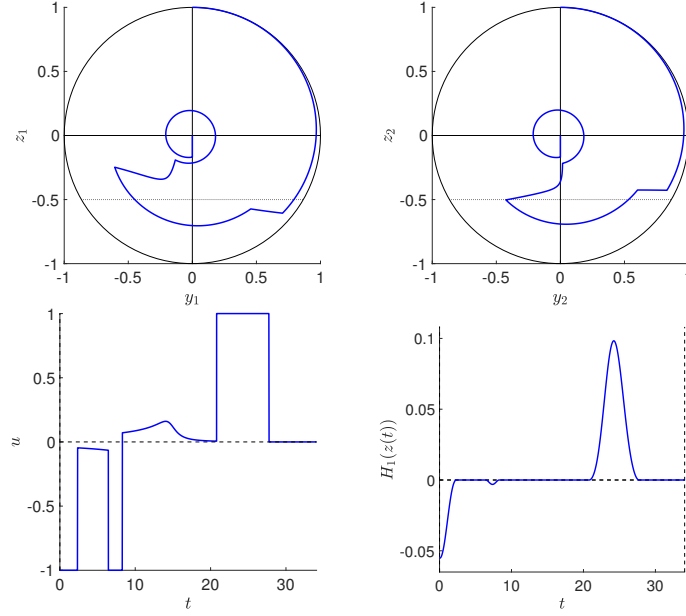

FIGURE 19. Fat case: $\rho = \bar{\rho}$, $\theta = 0.4636$ and $\varepsilon = 0.1$. Trajectories of spins 1 and 2, control and H_1.
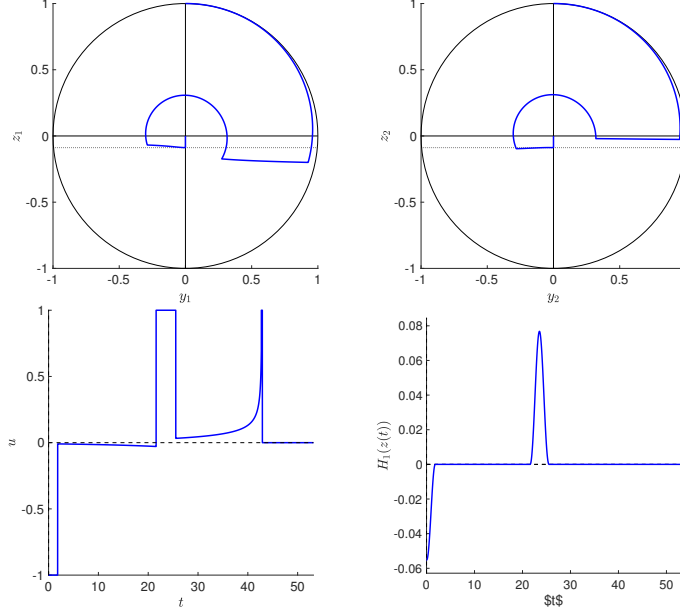
FIGURE 20. Fluid: $\rho = \bar{\rho}$, $\theta = 0.1489$ and $\varepsilon = 0.1$. Trajectories of spins 1 and 2, control and H_1.

Let us give now some details about the different homotopies. The first two paths (called H1a and H1b) are interesting since, even if they are distinct paths (see bottom-left subgraph of Fig 21), they intersect in terms of cost for a value $\theta^* \in [\theta_{1b,1}, \theta_{1b,2}]$, where $\theta_{1b,1} \approx 0.2752$ and $\theta_{1b,2} \approx 0.3018$. For $\theta \leq \theta^*$, H1b is better and for $\theta \geq \theta^*$, H1a is better, see top-left subgraph of Fig 21. The homotopy H1a has been already introduced in section 4.4.2. One starts from $\theta = \theta_{\max}$ with a structure of the form BSBS ($\sigma_-\sigma_s\sigma_+\sigma_0$). Around $\theta = \theta_{1a,1} \approx 0.5069$, the monitoring detects a change in the structure: a singular arc has to be added inside the first negative bang arc and the structure becomes $\sigma_-\sigma_s\sigma_-\sigma_s\sigma_+\sigma_0$. A new change occurs around $\theta_{1a,2} \approx 0.2722$: the second singular arc vanishes and the structure becomes $\sigma_-\sigma_s\sigma_-\sigma_+\sigma_0$. We stop the homotopy here since the homotopy H1b is better for this value of θ. Le us explain the homotopy H1b: this homotopy starts from $\theta = \theta_{\min}$ with a structure of the form BSBSBS ($\sigma_-\sigma_s\sigma_+\sigma_s\sigma_+\sigma_0$). A first change in the structure is detected around $\theta_{1b,1} \approx 0.2752$: the second singular arc vanishes and the structure becomes $\sigma_-\sigma_s\sigma_+\sigma_0$. A second change occurs around $\theta_{1b,2} \approx 0.3018$: the control saturates at the end of the first singular arc. We denote by σ_s^- this singular arc with since at the end the control takes the value -1. The structure is now $\sigma_-\sigma_s^-\sigma_+\sigma_0$ and we do not continue the homotopy since H1a is better for $\theta = \theta_{1b,2}$. The different structures with the names of the homotopies and the associated figures to observe the trajectories and the control are given in Table 4 and Figs. 22–36.

Let us give some details about the two last homotopies. The homotopy H2 starts with a local solution (not globally optimal, see top-right subgraph of Fig 21) of the form $\sigma_+\sigma_s\sigma_+\sigma_s\sigma_+\sigma_0$ for $\theta = 0.2$. This solution has the particularity that all the bang arcs are positive bang arcs. Besides, the trajectory (see Fig 29) has a self-intersection which prevents the BC-extremal to be globally optimal. During

the homotopy there is only one change, the first singular arc vanishes around $\theta = \theta_{2,1} \approx 0.3618$. This homotopy may be compared with the homotopy H3. The homotopy H3 is similar as H2 but the last bang arc is longer. During this last bang arc, the trajectory realizes a complete turn around its center. There is also one single change around $\theta = \theta_{2,1} \approx 0.4778$, from which the first singular arc vanishes.

Name	Init	Transition	End
H1a	$\theta_{\max} \approx 1.1071$ $\sigma_-\sigma_s\sigma_+\sigma_0$ fig 22	$\theta_{1a,1} \approx 0.5069$ $\sigma_-\sigma_s\sigma_-\sigma_s\sigma_+\sigma_0$ fig 23	$\theta_{1a,2} \approx 0.2722 > \theta_{\min} = 0.02$ $\sigma_-\sigma_s\sigma_-\sigma_+\sigma_0$ fig 24
H1b	$\theta_{\min}$ $\sigma_-\sigma_s\sigma_+\sigma_s\sigma_+\sigma_0$ fig 25	$\theta_{1b,1} \approx 0.2752$ $\sigma_-\sigma_s\sigma_+\sigma_0$ figs 26 and 27	$\theta_{1b,2} \approx 0.3018 < \theta_{\max}$ $\sigma_-\sigma_s^-\sigma_+\sigma_0$ fig 28
H2	$\theta = 0.2$ $\sigma_+\sigma_s\sigma_+\sigma_s\sigma_+\sigma_0$ fig 29	$\theta_{2,1} \approx 0.3618$ $\sigma_+\sigma_s\sigma_+\sigma_0$ figs 30 and 31	$\theta = \mathrm{atan}(1.5) \approx 0.9828$ $\sigma_+\sigma_s\sigma_+\sigma_0$ fig 32
H3	$\theta = 0.25$ $\sigma_+\sigma_s\sigma_+\sigma_s\sigma_+\sigma_0^1$ fig 33	$\theta_{3,1} \approx 0.4778$ $\sigma_+\sigma_s\sigma_+\sigma_0^1$ figs 34 and 35	$\theta = \theta_{\max}$ $\sigma_+\sigma_s\sigma_+\sigma_0^1$ fig 36

TABLE 4. The homotopies are detailed on each line. The first column gives the name of the homotopy. The second colum "Init" gives the initial value of θ, the associated structure with the reference to the figure which presents the trajectory with the control and the switching function. For this initial value, the solution is obtained from direct method and multiple shooting. The column "Transition" gives the same details but when a first change in the structure is detected during the homotopy thanks to the monitoring. The last column "End" gives again the same details at the end of the homotopy. For the homotopies H1a and H1b, the end occurs when a second change in the structure is detected while for H2 and H3, the end occurs when the final value of θ is reached. The red and green colors may help to understand the change in the structure, which is explained more in details in this section.
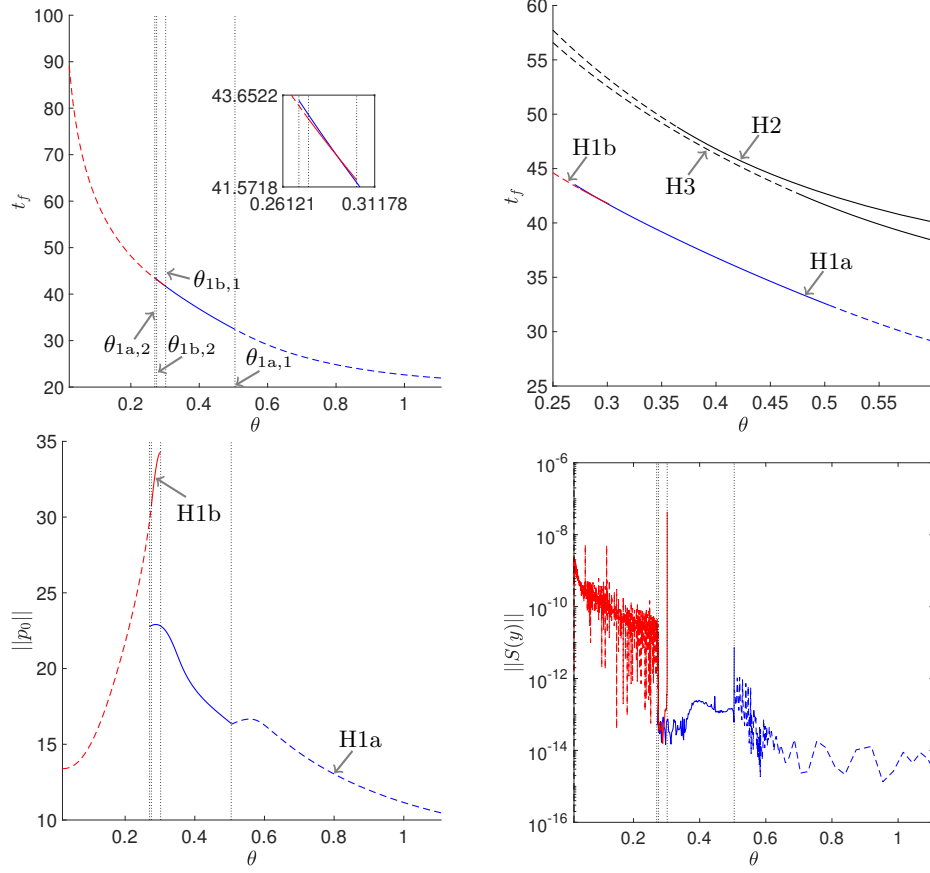
FIGURE 21. The homotopies H1a, H1b, H2 and H3 are presented respectively in blue, red, black and black. The homotopies H2 and H3 are presented only on the top-right subgraph. The plain and dashed lines distinguish the different structures. The top-left subgraph gives the cost (*i.e.* the final time t_f) with respect to θ for the homotopies H1a and H1b. One can see (it is more visible in the zoom) the intersection of the two paths of zeros in terms of cost. H1b is better for small value of θ and H1a is better for greater values. One can notice that this two paths of zeros are distinct from the bottom-left subgraph. This subgraph gives the norm of the initial adjoint vector with respect to the homotopic parameter. The norm of the shooting function along the paths H1a and H1b is given in the bottom-left subgraph. One can see the very good accuracy. The strategies from H1a and H1b are compared with homotopies H2 and H3 on the top-right subgraph.
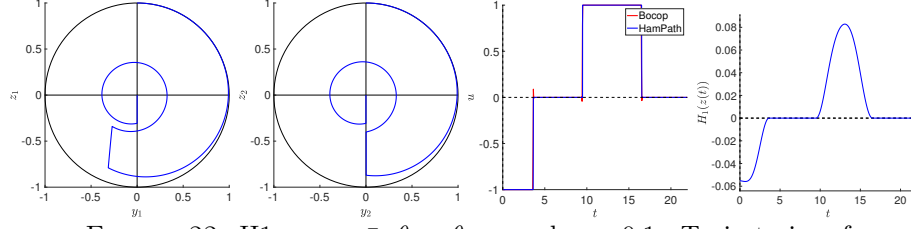
FIGURE 22. H1a: $\rho = \bar{\rho}$, $\theta = \theta_{\max}$ and $\varepsilon = 0.1$. Trajectories of spins 1 and 2, control and H_1.
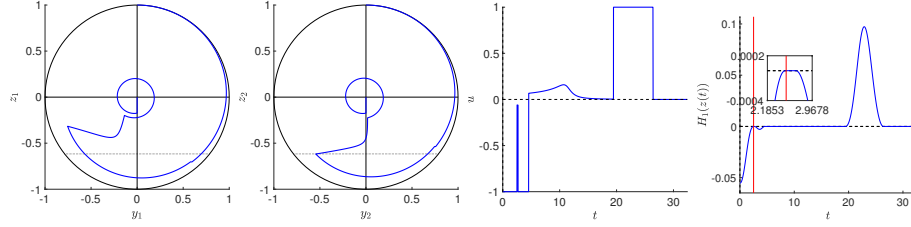

FIGURE 23. H1a: $\rho = \bar{\rho}$, $\theta = \theta_{1a,1}^-$ and $\varepsilon = 0.1$. Trajectories of spins 1 and 2, control and H_1.

FIGURE 24. H1a: $\rho = \bar{\rho}$, $\theta = \theta_{1a,2}^+$ and $\varepsilon = 0.1$. Trajectories of spins 1 and 2, control and H_1.

FIGURE 25. H1b: $\rho = \bar{\rho}$, $\theta = \theta_{\min}$ and $\varepsilon = 0.1$. Trajectories of spins 1 and 2, control and H_1.

FIGURE 26. H1b: $\rho = \bar{\rho}$, $\theta = \theta_{1b,1}^-$ and $\varepsilon = 0.1$. Trajectories of spins 1 and 2, control and H_1.

FIGURE 27. H1b: $\rho = \bar{\rho}$, $\theta = \theta_{1b,1}^+$ and $\varepsilon = 0.1$. Trajectories of spins 1 and 2, control and H_1.
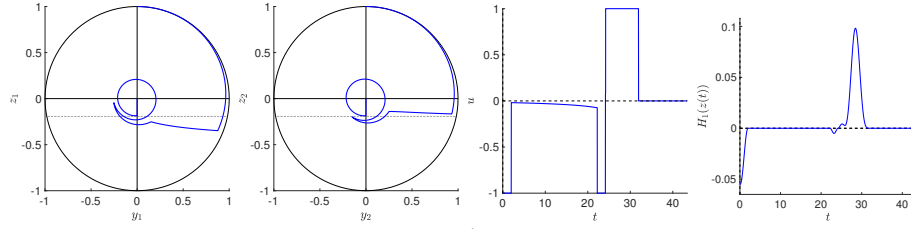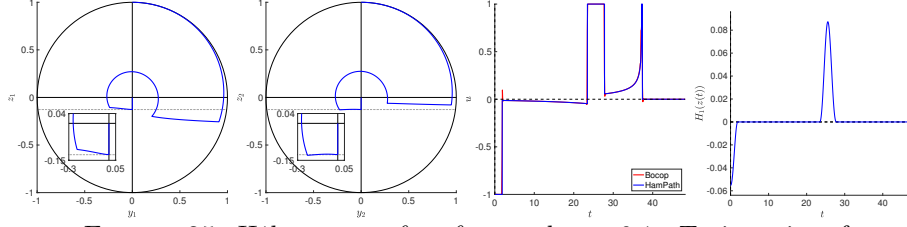
FIGURE 28. H1b: $\rho = \bar{\rho}$, $\theta = \theta_{1b,2}^+$ and $\varepsilon = 0.1$. Trajectories of spins 1 and 2, control and H_1.

FIGURE 29. H2: $\rho = \bar{\rho}$, $\theta = 0.2$ and $\varepsilon = 0.1$. Trajectories of spins 1 and 2, control and H_1.
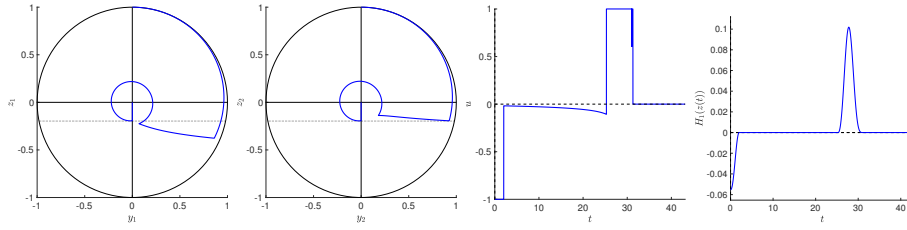
FIGURE 30. H2: $\rho = \bar{\rho}$, $\theta = \theta_{2,1}^-$ and $\varepsilon = 0.1$. Trajectories of spins 1 and 2, control and H_1.

FIGURE 31. H2: $\rho = \bar{\rho}$, $\theta = \theta_{2,1}^+$ and $\varepsilon = 0.1$. Trajectories of spins 1 and 2, control and H_1.

FIGURE 32. H2: $\rho = \bar{\rho}$, $\theta = \mathrm{atan}(1.5)$ and $\varepsilon = 0.1$. Trajectories of spins 1 and 2, control and H_1.

FIGURE 33. H3: $\rho = \bar{\rho}$, $\theta = 0.25$ and $\varepsilon = 0.1$. Trajectories of spins 1 and 2, control and H_1.

FIGURE 34. H3: $\rho = \bar{\rho}$, $\theta = \theta_{3,1}^-$ and $\varepsilon = 0.1$. Trajectories of spins 1 and 2, control and H_1.
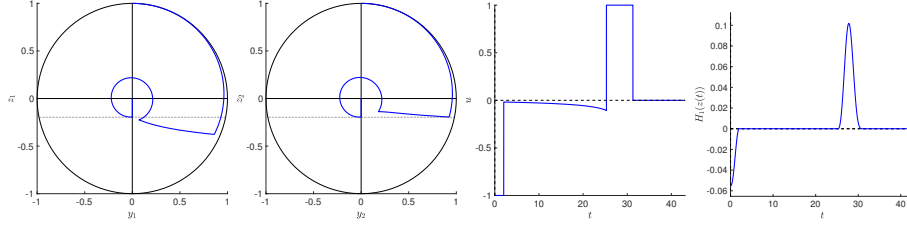
FIGURE 35. H3: $\rho = \bar{\rho}$, $\theta = \theta_{3,1}^+$ and $\varepsilon = 0.1$. Trajectories of spins 1 and 2, control and H_1.
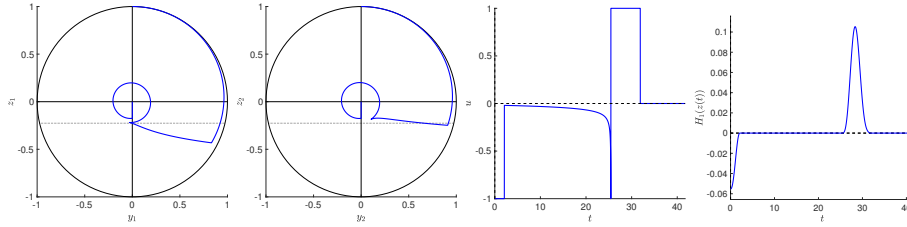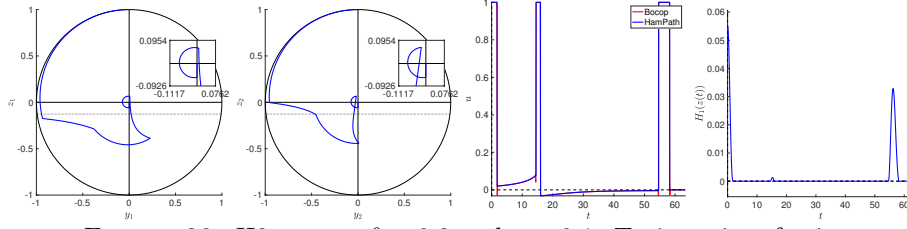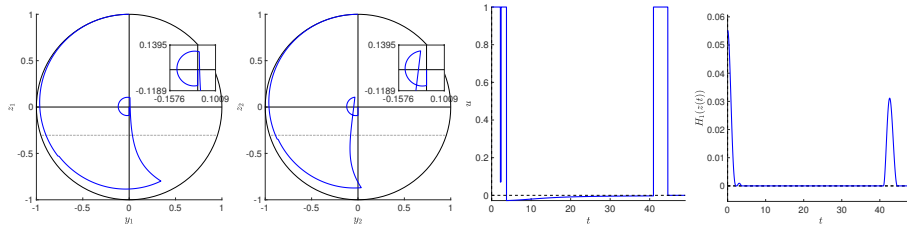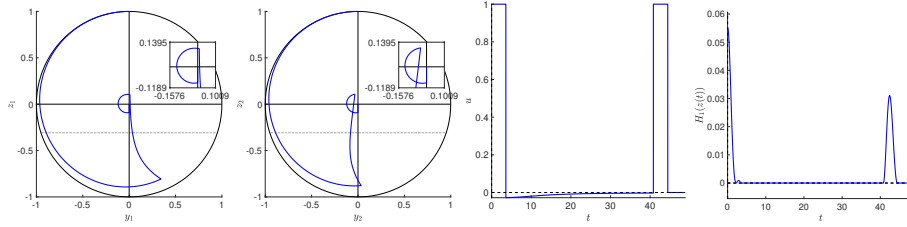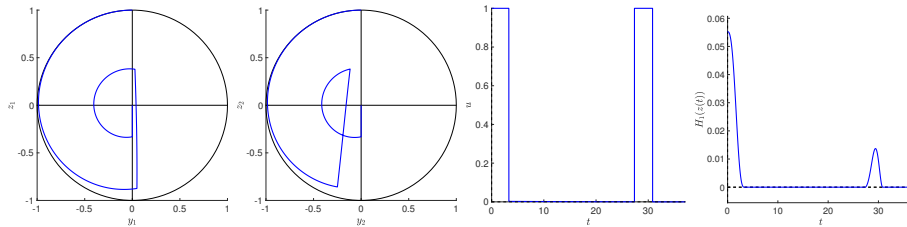
FIGURE 36. H3: $\rho = \bar{\rho}$, $\theta = \mathrm{atan}(2)$ and $\varepsilon = 0.1$. Trajectories of spins 1 and 2, control and H_1.
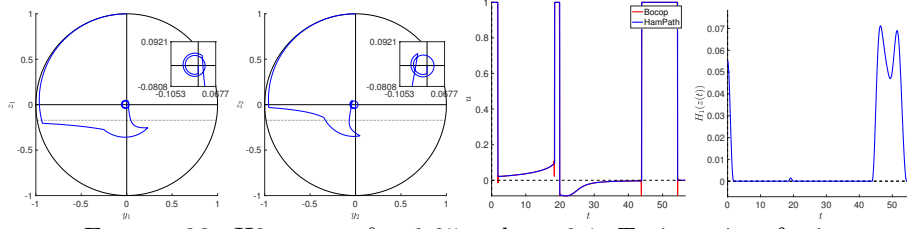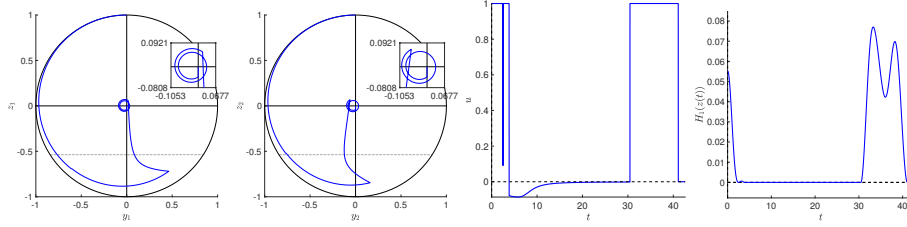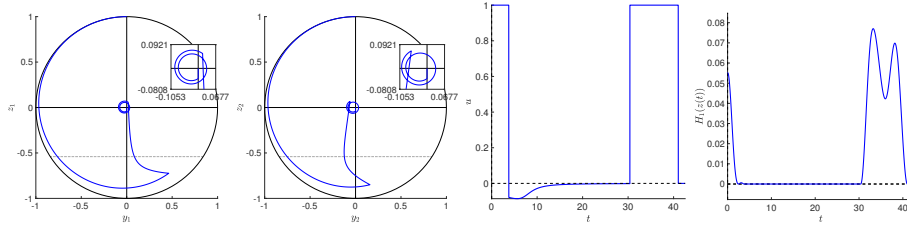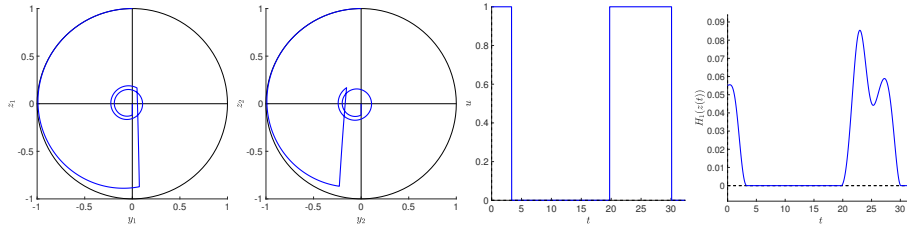
5. Algebraic computations for multisaturation with B_1-inhomogeneity

The `Maple` symbolic software is used to perform algebraic computations related to singularity analysis of the extremal trajectories, in particular in relation with the determination of bridges. The computations boiled down to compute Gröbner basis and one needs the following concepts and techniques of this area.

5.1. Operation on polynomial ideals.

Let n be a positive integer and we consider polynomials in $A = \mathbb{C}[X_1, \ldots, X_n]$. Given a system of equations $\mathcal{F}$, one consider the ideal I coding the set $V(\mathcal{F}$ of zeros of $\mathcal{F}$.

Given an ideal J and a polynomial F, saturating I by F means computing a set of generators of the ideal

$$(I : F^\infty) = \{ g \in A, \ \exists m \in \mathbb{N}, \ gF^m \in I \}.$$

The radical of an ideal I is the set:

$$\sqrt{I} = \{ f \in A, \ \exists m \in \mathbb{N}, \ f^m \in I \}$$

and it has the same set of zeros. An operation used given a set of generators of I, computing a set of generators of $J \supset I$ such that $\sqrt{I} = \sqrt{J}$. This can be done by using the square free form of the generators: give a polynomial f with decomposition in primes $p_1^{n_1} \ldots p_r^{n_r}$, the square free form is $sqfr(f) = p_1 \ldots p_r$.

5.2. Frame curves.

Frame curves associated to the saturation of a single spin lead to the following.

- *Collinearity locus:* $\mathcal{C}$ is defined as the set where f and g are linearly dependent. Outside zero it is defined by: $\exists \lambda$ such that $F = \lambda G$ that is:

$$-\Gamma y_1 = \lambda z_1, \quad \gamma(1 - z_1) = \lambda y_1,$$
$$-\Gamma y_2 = \lambda z_2 (1 - \varepsilon), \quad \gamma(1 - z_2) = \lambda y_2 (1 - \varepsilon),$$

  The projections on q_i-spaces are the ovals:

$$\Gamma_i y_i^2 = \gamma (1 - z_i) z_i, \quad 0 \le z_i \le 1, \quad i = 1, 2$$

  intersected with one of the sets

$$\Gamma(1 - \varepsilon) y_1 z_2 = \Gamma y_2 z_1, \quad (1 - \varepsilon) y_2 (1 - z_1) = y_1 (1 - z_2)$$

- *Singularity locus:* $\mathcal{S}$ is defined as the set where G and $[F, G]$ are linearly independent. Outside zero it is defined by: $\exists \lambda$ such that $[F, G] = \lambda G$, that is

$$\delta z_1 - \gamma = -\lambda z_1, \quad \delta y_1 = \lambda y_1,$$
$$\delta z_2 - \gamma = -\lambda z_2, \quad \delta y_2 = \lambda y_2,$$

  Projections on each q_i-spaces will form the two singular lines

$$z_s^i = \gamma / 2\delta, \quad y_i = 0, \quad i = 1, 2.$$

  The additional relations defined the full locus.

5.3. Singularity classification: exceptional case $H_F = 0$.

Conventions and notations. For the computations, we use the translation

$$z_1 \leftarrow z_1 + 1, \; z_2 \leftarrow z_2 + 1, \tag{5.1}$$

which places the center of the coordinates at the North pole of the Bloch ball. In this new system of coordinates, the center of the Bloch ball has coordinates $(0, -1, 0, -1)$.

We have in the exceptional case the constraint

$$p \cdot F = p \cdot G = p \cdot [F, G] = 0,$$

hence p can be eliminated in the relation defining the control

$$p \cdot ([[G, F], F] + u\,[[G, F], G]) = 0$$

which is computed as the feedback

$$u_s(q) = -\frac{D'(q)}{D(q)}$$

with

$$D = \det(F, G, [G, F], [[G, F], G])$$

$$\tag{5.2}$$

$$= \det \begin{bmatrix} -\Gamma y & -z - 1 & \delta z - \Gamma & 2\delta y \\ -\gamma z & y & \delta y & -2\delta z + \Gamma - \delta \\ -\Gamma y & (1 - \epsilon)(-z - 1) & (1 - \epsilon)(\delta z - \Gamma) & (1 - \epsilon)^2(2\delta y) \\ -\gamma z & (1 - \epsilon)y & (1 - \epsilon)\delta y & (1 - \epsilon)^2(-2\delta z + \Gamma - \delta) \end{bmatrix}$$

and

$$D' = \det(F, G, [G, F], [[G, F], F])$$

$$\tag{5.3}$$

$$= \begin{bmatrix} -\Gamma y & -z - 1 & \delta z - \Gamma & \gamma(\gamma - 2\Gamma) + \delta^2(z + 1) \\ -\gamma z & y & \delta y & \delta^2 y \\ -\Gamma y & (1 - \epsilon)(-z - 1) & (1 - \epsilon)(\delta z - \Gamma) & (1 - \epsilon)^2(\gamma(\gamma - 2\Gamma) + \delta^2(z + 1)) \\ -\gamma z & (1 - \epsilon)y & (1 - \epsilon)\delta y & (1 - \epsilon)^2\delta^2 y \end{bmatrix}$$

Using a time reparameterization, this leads to analyze the C^ω-vector field in the q-space

$$X = DF - D'G.$$

The following polynomials will appear frequently in the remainder of the section:

- $P_{y_1} := y_1 - (1 - \epsilon)y_2$
- $P_{y_2} := y_2 - (1 - \epsilon)y_1$
- $P_{z_1} := 2(\Gamma - \gamma)z_1 + 2\Gamma - \gamma$
- $P_{z_2} := 2(\Gamma - \gamma)z_2 + 2\Gamma - \gamma$

The root of the univariate polynomials P_{z_1} and P_{z_2} is

$$z_S = \frac{\gamma - 2\Gamma}{2\Gamma - 2\gamma}. \tag{5.4}$$

5.3.1. *Transfer time not fixed ($H_F = 0$).*

$$\left\langle D, \frac{\partial D}{\partial y_1}, \frac{\partial D}{\partial y_2}, \frac{\partial D}{\partial z_1}, \frac{\partial D}{\partial z_2} \right\rangle$$

$$\left\langle \tilde{D}, \frac{\partial \tilde{D}}{\partial y_1}, \frac{\partial \tilde{D}}{\partial y_2}, \frac{\partial \tilde{D}}{\partial z_1}, \frac{\partial \tilde{D}}{\partial z_2} \right\rangle$$

$z_2 = 0$

$\begin{aligned} P_{z_2} &= 0 \\ z_2 &\neq 0 \end{aligned}$

$z_1 = 0$
$y_2 = 0$
$y_1 = 0$

$z_1 = z_2$

$y_1 = 0 \qquad P_{y_1} = 0$
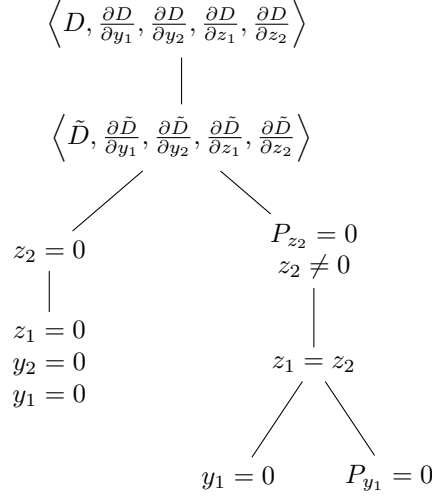
FIGURE 37. Structure of the study of the singularities of $\{D = 0\}$

Singularities of $\{D = 0\}$.

Proposition 5.1. *The set of points satisfying $D = \frac{\partial D}{\partial y_1} = \frac{\partial D}{\partial z_1} = \frac{\partial D}{\partial y_2} = \frac{\partial D}{\partial z_2} = 0$ is given, generically on authorized values of γ, Γ, by*

(1) *the point $y_1 = y_2 = z_1 = z_2 = 0$, and*
(2) *the curve defined by $P_{y_1} = P_{z_1} = P_{z_2} = 0$, which is parameterized by y_2 as*

$$\begin{cases} y_1 = (1 - \epsilon)y_2 \\ z_1 = z_2 = z_S = \frac{\gamma - 2\Gamma}{2\Gamma - 2\gamma}. \end{cases} \tag{5.5}$$

If $\gamma = \Gamma$ (for example if the matter is water), only the former solution exists.

Proof. The structure of this proof is summarized in Fig. 37. The determinant D can be factored as $(1 - \epsilon)\tilde{D}$. The singularities of D and those of $\tilde{D}$ are the same, so for the study, we consider the ideal

$$I := \left\langle \tilde{D}, \frac{\partial \tilde{D}}{\partial y_1}, \frac{\partial \tilde{D}}{\partial y_2}, \frac{\partial \tilde{D}}{\partial z_1}, \frac{\partial \tilde{D}}{\partial z_2} \right\rangle. \tag{5.6}$$

In order to eliminate y_1, y_2 and z_1 from the ideal I, we compute a Gröbner basis $\mathcal{G}$ of I with respect to the elimination ordering $y_1 > y_2 > z_1 \gg z_2 > \epsilon > \Gamma > \gamma$. This computation yields that

$$I \cap \mathbb{Q}[z_2, \epsilon, \Gamma, \gamma] = \left\langle \epsilon^2(\epsilon - 2)^2(2\Gamma - \gamma)(\Gamma - \gamma)z_2^3 P_{z_2}^3 \right\rangle, \tag{5.7}$$

so singular points necessarily satisfy

$$\begin{cases} z_2 = 0 \\ \quad \text{or} \\ P_{z_2} = 0 \iff z_2 = \frac{\gamma - 2\Gamma}{2\Gamma - 2\gamma}. \end{cases} \tag{5.8}$$

If $\Gamma = \gamma$ (that is, if the matter is water), the second of these solutions does not exist. If $\gamma = 2\Gamma$ (which means that the matter is on the limit of the domain of validity $2\Gamma \geq \gamma$), both solutions coincide.

In all other cases, there are 2 distinct possible values for z_2, and we consider both cases: we consider the two ideals

$$I_1 := \langle \mathsf{sqfr}(\mathcal{G}), z_2 \rangle \tag{5.9}$$

$$I_2 := \langle \mathsf{sqfr}(\mathcal{G}), P_{z_2} \rangle \tag{5.10}$$

where for any polynomial f, $\mathsf{sqfr}(f)$ is the square-free part of f and $\mathsf{sqfr}(\mathcal{G})$ means that we apply sqfr to each element of $\mathcal{G}$.

In order to lift the partial solution $z_2 = 0$, we compute a Gröbner basis $\mathcal{G}_1$ of I_1 with respect to the ordering $y_1 > y_2 \gg z_1 > z_2 > \epsilon > \Gamma > \gamma$, and we find that this ideal contains

$$\gamma z_1^2 (\epsilon - 1)^2 (2\Gamma - \gamma), \tag{5.11}$$

so $z_1 = 0$.

We then compute a Gröbner basis of $\langle \mathsf{sqfr}(\mathcal{G}_1), z_1 \rangle$ with respect to the order $y_1 \gg y_2 > z_1 > z_2 > \epsilon > \Gamma > \gamma$, and we find that this ideal contains

$$\Gamma \gamma \epsilon y_2^2 (\Gamma - \gamma)(2\Gamma - \gamma)^2 (\epsilon - 2), \tag{5.12}$$

so $y_2 = 1$.

Finally, adding y_2 to the ideal yields that

$$0 = \Gamma y_1 (\epsilon - 1)(2\Gamma - \gamma), \tag{5.13}$$

so the final solution is

$$(y_1, y_2, z_1, z_2) = (0, 0, 0, 0). \tag{5.14}$$

We now consider the partial solution $z_2 = (\gamma - 2\Gamma)/(2\Gamma - 2\gamma)$. We compute a Gröbner basis $\mathcal{G}_2$ of I_2 with respect to the order $y_1 > y_2 \gg z_1 > z_2 > \epsilon > \Gamma > \gamma$, and we find that the ideal contains

$$z_2 \gamma (z_1 - z_2)^2. \tag{5.15}$$

Since this case was already studied, we may assume that $z_2 \neq 0$, so

$$z_1 = z_2 = \frac{\gamma - 2\Gamma}{2\Gamma - 2\gamma}. \tag{5.16}$$

Adding $z_1 - z_2$ to $\mathsf{sqfr}(\mathcal{G}_2)$ and computing a Gröbner basis for the order $y_1 \gg y_2 > z_1 > z_2 > \epsilon > \Gamma > \gamma$, we find that the ideal contains

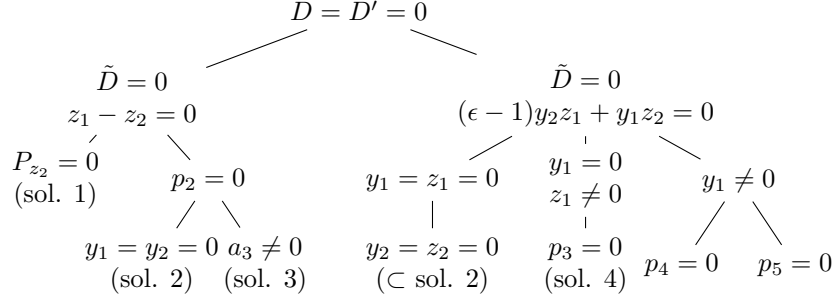$$\gamma^2 y_2 (\epsilon - 1) P_{y_1} (2\Gamma - \gamma), \tag{5.17}$$

so we have 2 new branches to consider.

If $y_2 \neq 0$, $y_1 = (1 - \epsilon) y_2$. Otherwise, by adding $y_2 = 0$ to the system of equations, we find that the ideal contains

$$\gamma y_1^2 z_2, \tag{5.18}$$

so $y_1 = 0$, and in particular, this point is on $\{P_{y_1} = 0\}$.

$\square$

$$D = D' = 0$$

$$\tilde{D} = 0$$
$$z_1 - z_2 = 0$$

$$\tilde{D} = 0$$
$$(\epsilon - 1)y_2 z_1 + y_1 z_2 = 0$$

$P_{z_2} = 0$
(sol. 1)

$p_2 = 0$

$y_1 = z_1 = 0$

$y_1 = 0$
$z_1 \neq 0$

$y_1 \neq 0$

$y_1 = y_2 = 0$ $a_3 \neq 0$
(sol. 2)   (sol. 3)

$y_2 = z_2 = 0$
($\subset$ sol. 2)

$p_3 = 0$
(sol. 4)

$p_4 = 0$ $p_5 = 0$

FIGURE 38. Structure of the study of $\{D = D' = 0\}$

Locus of $\{D = D' = 0\}$.

Proposition 5.2. *The points of $\{D = D' = 0\}$ are given by:*

(1) *the plane*

$$z_1 = z_2 = z_S = \frac{\gamma - 2\Gamma}{2\Gamma - 2\gamma} \tag{5.19}$$

(2) *the line*

$$\begin{cases} y_1 = y_2 = 0 \\ z_1 = z_2 \end{cases} \tag{5.20}$$

(3) *the surface (parameterized by y_1, y_2)*

$$z_1 = z_2 = \frac{\Gamma P_{y_2}^2 (\gamma - 2\Gamma)}{2(\Gamma - \gamma)a_3} \tag{5.21}$$

    with

$$a_3 = (\Gamma + \gamma)P_{y_1}^2 + \epsilon(\epsilon - 2)\Gamma(y_1 - y_2)(y_1 + y_2) \tag{5.22}$$

(4) *the surface (parameterized by y_1, z_2)*

$$y_2 = \frac{y_1 z_2}{(1 - \epsilon)z_1}, \quad z_1 = \frac{(2\Gamma - \gamma)z_2}{a_4} \tag{5.23}$$

    with

$$a_4 = 2(\epsilon - 2)(\Gamma - \gamma)\epsilon z_2 + (2\Gamma - \gamma)(\epsilon - 1)^2 \tag{5.24}$$

(5) *the surface (parameterized by y_2, z_2)*

$$z_1 = \frac{z_2 y_1}{(1 - \epsilon)y_2}, \quad y_1 = \frac{(1 - \epsilon)y_2 \left((2\Gamma - \gamma)\Gamma y_2^2 + \gamma^2 z_2^2\right)}{a_5} \tag{5.25}$$

    with

$$a_5 = \Gamma \left(2\epsilon(\epsilon - 2)(\Gamma - \gamma)z_2 + (\epsilon - 1)^2(2\Gamma - \gamma)\right) y_2^2 + \gamma^2 z_2^2 \tag{5.26}$$

Proof. The structure of this proof is summarized in Fig. 38. The determinant D' factors as

$$D' = 2\gamma^2(2\Gamma - \gamma)(\Gamma - \gamma)(z_1 - z_2)(\epsilon - 1)((\epsilon - 1)y_2 z_1 + y_1 z_2), \tag{5.27}$$

so we form the two ideals

$$I_1 = \langle \tilde{D}, z_1 - z_2 \rangle \tag{5.28}$$

$$I_2 = \langle \tilde{D}, (\epsilon - 1)y_2 z_1 + y_1 z_2 \rangle. \tag{5.29}$$

If $z_1 = z_2$, after substitution, $\tilde{D}$ has two factors depending on y_1, y_2, z_2: P_{z_2} and

$$p_2 := 2(\Gamma - \gamma)\left((\Gamma + \gamma)P_{y_1}^2 + \epsilon(\epsilon - 2)\Gamma(y_1 - y_2)(y_1 + y_2)\right)z_2 + \Gamma P_{y_2}^2(2\Gamma - \gamma) \tag{5.30}$$

The polynomial P_{z_2} gives solution 1.

Let

$$a_3(y_1, y_2) = (\Gamma + \gamma)P_{y_1}^2 + \epsilon(\epsilon - 2)\Gamma(y_1 - y_2)(y_1 + y_2) \tag{5.31}$$

so that the coefficient of z_2 in p_2 is $2(\Gamma - \gamma)a_3$, it is homogeneous in y_1, y_2 with degree 2. Its discriminant in y_2 is

$$-4(\epsilon - 2)^2 \epsilon^2 y_1^2 \gamma \Gamma. \tag{5.32}$$

Since the parameters γ, Γ are necessarily positive, this discriminant is negative, and thus the only real root of $a_3(y_1, y_2)$ is $y_1 = y_2 = 0$. If $y_1 = y_2 = 0$, p_2 vanishes regardless of z_2.

If $y_1 \neq 0$, $a_3(y_1, y_2)$ does not have any real root in y_2, and z_2 is given by

$$(z_1 =)z_2 = \frac{\Gamma P_{y_2}^2 (\gamma - 2\Gamma)}{2(\Gamma - \gamma)a_3(y_1, y_2)}. \tag{5.33}$$

We now turn to the other branch, defined by $(\epsilon - 1)y_2 z_1 + y_1 z_2 = 0$.

If $y_1 = z_1 = 0$, there are 2 curves of singular points defined (in y_2, z_2) by

$$\Gamma(2\Gamma - \gamma)y_2^2 + \gamma^2 z_2^2 = 0. \tag{5.34}$$

Since $2\Gamma \geq \gamma$, the only solution is $z_2 = 0$ with either $2\Gamma = \gamma$ or $y_2 = 0$.

If $y_1 = 0$ and $z_1 \neq 0$, then (since $\epsilon \neq 1$) we must have $y_2 = 0$. Furthermore, we may assume that $z_1 \neq z_2$ since this case was already studied. The remaining solutions form a curve defined by

$$0 = p_3 := \left(2(\epsilon - 2)(\Gamma - \gamma)\epsilon z_2 + (2\Gamma - \gamma)(\epsilon - 1)^2\right)z_1 - (2\Gamma - \gamma)z_2. \tag{5.35}$$

Let $a_4(z_1, z_2)$ be the coefficient of z_1 in p_3, the solutions are given by either

$$\begin{cases} a_4(z_2) \neq 0 \\ z_1 = \dfrac{2\Gamma - \gamma}{c_3(z_2)}z_2 \end{cases} \tag{5.36}$$

or (since by assumption $z_1 \neq 0$)

$$z_2 = 2\Gamma - \gamma = 0. \tag{5.37}$$

So we may assume that $y_1 \neq 0$. We compute a Gröbner basis of $I_2 + \langle uy_1 - 1 \rangle$ for the order $u \gg z_1 > y_1 \gg z_2 > y_2 > \epsilon > \gamma > \Gamma$. This basis contains a polynomial which factors as the product of

$$p_4 = \left(2(\epsilon - 2)(\Gamma - \gamma)\epsilon z_2 + (\epsilon - 1)^2(2\Gamma - \gamma)\right)y_1 + (\epsilon - 1)(2\Gamma - \gamma)y_2 \tag{5.38}$$

and

$$\begin{aligned} p_5 = &\left(\Gamma\left(2\epsilon(\epsilon - 2)(\Gamma - \gamma)z_2 + (\epsilon - 1)^2(2\Gamma - \gamma)\right)y_2^2 + \gamma^2 z_2^2\right)y_1 \\ &+ (\epsilon - 1)y_2\left((2\Gamma - \gamma)\Gamma y_2^2 + \gamma^2 z_2^2\right). \end{aligned} \tag{5.39}$$

First, assume that $p_4 = 0$. We compute a Gröbner basis of $I_2 + \langle uy_1 - 1, p_4 \rangle$ for the order $u \gg z_1 > y_1 \gg z_2 > y_2 > \epsilon > \gamma > \Gamma$, and we find that the last polynomial defining the ideal is p_3, whose solutions we already studied.

Finally, assume that $p_4 \neq 0$ and $p_5 = 0$. The discriminant in y_2 of the coefficient $a_5(y_2, z_2)$ of y_1 in p_5 is

$$- 4a_4(z_2)\Gamma\gamma^2 z_2^2 \tag{5.40}$$

where $a_4(z_2)$ is as above the coefficient of z_1 in p_3. The last components of the solutions are given by

$$\begin{cases} a_5(y_2, z_2) \neq 0 \\ y_1 = \frac{(1-\epsilon)y_2\left((2\Gamma-\gamma)\Gamma y_2^2 + \gamma^2 z_2^2\right)}{\Gamma(2\epsilon(\epsilon-2)(\Gamma-\gamma)z_2 + (\epsilon-1)^2(2\Gamma-\gamma))y_2^2 + \gamma^2 z_2^2} \end{cases} \tag{5.41}$$

and

$$\begin{cases} a_5(y_2, z_2) = 0 \\ y_2\left((2\Gamma - \gamma)\Gamma y_2^2 + \gamma^2 z_2^2\right) \end{cases} \tag{5.42}$$

which, as in the case $y_1 = z_1 = 0$, is only $y_2 = z_2 = 0$ if $2\Gamma > \gamma$. This partial solution completes into $y_1 = y_2 = z_1 = z_2 = 0$, which was already known. □

Equilibrium positions.

Lemma 5.3. *The equilibrium points of $\dot{X} = DF - D'G$ are all contained in $\{D = D' = 0\}$.*

Proof. Assume that at some point, either of the determinants D and D' is non-zero, this implies that F and G are colinear. Since F and G form the first two columns of the matrices whose D and D' are the respective determinants, $D = D' = 0$ at that point. □

Linearization of the system at equilibrium points. For each of the components of the set of equilibrium points $\{D = D' = 0\}$ found in the previous paragraph, we inspect the behavior of the system in a neighborhood. Namely, for each equilibrium point q, we write

$$\frac{\mathrm{d}}{\mathrm{d}t}(q + \delta q) = (DF - D'G)(q) + A(q) \cdot \delta q + R(\delta q). \tag{5.43}$$

where $A = \mathrm{Jac}_q(DF - D'G)$, so that

$$\frac{\mathrm{d}}{\mathrm{d}t}(\delta q) = A(q) \cdot \delta q + R(q)(\delta q). \tag{5.44}$$

We can compute $A(q)$ explicitly: Indeed, let $f = DF - D'G$. Its first derivative is

$$\mathrm{d}f(q)(u) = \mathrm{d}D(q)(u)F(q) + D(q)\mathrm{d}F(q)(u) - \mathrm{d}D'(q)(u)G(q) - D'(q)\mathrm{d}G(q)(u), \tag{5.45}$$

so

$$A(q) = \nabla D(q).F(q) + D(q)\mathrm{Jac}_q(F)(q) - \nabla D'(q).G(q) - D'(q)\mathrm{Jac}_q(G)(q). \tag{5.46}$$

We examine the eigenvalue decomposition of $A(q)$.

Solution 1 (5.19). If $z_1 = z_2 = \frac{\gamma - 2\Gamma}{2\Gamma - 2\gamma}$, the characteristic polynomial of A factors as

$$T^2 \left(T - \gamma^2(2\Gamma - \gamma)^2(\epsilon - 1)P_{y_1}^2\right)^2 \tag{5.47}$$

The matrix $A(q)$ is diagonalizable.

Solution 2 (5.20). If $y_1 = y_2 = 0$ and $z_1 = z_2$, the characteristic polynomial of $A(q)$ is

$$T^4 \tag{5.48}$$

The Jacobian matrix $A(q)$ can be trigonalized as

$$A(q) = P^{-1} \begin{bmatrix} 0 & 1 & 0 & 0 \\ 0 & 0 & 0 & 0 \\ 0 & 0 & 0 & 0 \\ 0 & 0 & 0 & 0 \end{bmatrix} P \tag{5.49}$$

with the transition matrix

$$P = \begin{bmatrix} 0 & 1 & -1 & 0 \\ \epsilon\gamma^3(\epsilon-1)(\epsilon-2)z_1^2 P_{z_1} & 1 & 0 & 0 \\ 0 & 1 & 0 & 1 \\ \epsilon\gamma^3(\epsilon-1)(\epsilon-2)z_1^2 P_{z_1} & 0 & 0 & 0 \end{bmatrix}. \tag{5.50}$$

Solution 3 (5.21). If $z_1 = z_2 = \Gamma P_{y_2}^2(\gamma - 2\Gamma)/2(\Gamma - \gamma)a_3$, the characteristic polynomial of $A(q)$ factors as

$$T^2 \left(T + \frac{b_3}{a_3}\right)\left(T - \frac{b_3}{a_3}\right) \tag{5.51}$$

with

$$b_3 = \Gamma\gamma^2(\epsilon - 1)P_{y_1}P_{y_2}(2\Gamma - \gamma)^2. \tag{5.52}$$

The matrix $A(q)$ is diagonalizable.

Solution 4 (5.23). If $y_2 = \frac{y_1 z_2}{(1-\epsilon)z_1}$ and $z_1 = \frac{(2\Gamma-\gamma)z_2}{a_4}$, the characteristic polynomial of $A(q)$ factors as

$$T^2 \left(T - \frac{b_4}{a_4}\right)\left(T + \frac{b_4}{a_4}\right) \tag{5.53}$$

with

$$b_4 = 2\epsilon^2\gamma^3 z_2^3(\epsilon - 1)(\epsilon - 2)^2(2\Gamma - \gamma)(\Gamma - \gamma)P_{z_2}. \tag{5.54}$$

The matrix $A(q)$ is diagonalizable.

Solution 5 (5.25). If $z_1 = \frac{z_2 y_1}{(1-\epsilon)y_2}$ and $y_1 = \frac{(1-\epsilon)y_2\left((2\Gamma-\gamma)\Gamma y_2^2 + \gamma^2 z_2^2\right)}{a_5}$, the characteristic polynomial of $A(q)$ factors as

$$T^2 \left(T - \frac{b_4(\Gamma y_2^2 + \gamma(z_2^2 + z_2))\Gamma y_2^2}{a_5}\right)^2. \tag{5.55}$$

The matrix $A(q)$ is diagonalizable.

Special points. There are two points at which A vanishes: the North pole $N = (0,0,0,0)$ and $S = (0, z_S, 0, z_S)$. Both points are such that $D = D' = 0$, $\nabla D = \nabla D' = 0$, and additionally, at the North pole, $F(N) = 0$.

The North pole is on solutions 2, 3, 4 and 5.

The remainder at N is cubic:

$$\frac{\mathrm{d}}{\mathrm{d}t}(N + \delta q) = R(N)(\delta q) = O(\|\delta q\|^3). \tag{5.56}$$

The point S is the intersection of solutions 1 and 2. The remainder at S is quadratic.

Higher order studies for the special points.

Quadratic approximation at S**.** We now study the quadratic component $H_2 = Q(S)$ of the remainder $R(S)$:

$$\frac{\mathrm{d}}{\mathrm{d}t}(q + \delta q) = (DF - D'G)(q) + A(q)(\delta q) + Q(q)(\delta q) + O(\|\delta q\|^3), \qquad (5.57)$$

with $\frac{\mathrm{d}q}{\mathrm{d}t}(S) = (DF - D'G)(S) = 0$ and $A(S) = 0$.

We can compute Q by differentiating $f = DF - D'G$ again, as was done in [6, Sec. 3.4]. Differentiating (5.45) along q again, the second derivative of f is

$$\mathrm{d}^2 f(q)(u, v) = \mathrm{d}^2 D(q)(u, v)F(q) + \mathrm{d}D(q)(u)\mathrm{d}F(q)(v) + \mathrm{d}D(q)(v)\mathrm{d}F(q)(u)$$
$$- \mathrm{d}^2 D'(q)(u, v)G(q) - \mathrm{d}D'(q)(u)\mathrm{d}G(q)(v) - \mathrm{d}D'(q)(v)\mathrm{d}G(q)(u) \quad (5.58)$$

Note that second derivatives of F and G are 0, since their coordinates are affine in q.

We wish to compute $H_2(\delta q) = Q(S)(\delta q, \delta q) = \frac{1}{2}\mathrm{d}^2 f(q)(\delta q, \delta q)$. Since $\mathrm{d}D(S) = \mathrm{d}D'(S) = 0$, we find in the end that

$$H_2(\delta q) = h_2(\delta q)F(S) - h_2'(\delta q)G(S), \qquad (5.59)$$

with

$$F(S) = \left(0, \frac{\gamma(2\Gamma - \gamma)}{2(\Gamma - \gamma)}, 0, \frac{\gamma(2\Gamma - \gamma)}{2(\Gamma - \gamma)}\right)^t$$
$$\qquad (5.60)$$

$$G(S) = \left(\frac{\gamma}{2(\Gamma - \gamma)}, 0, \frac{(1 - \epsilon)\gamma}{2(\Gamma - \gamma)}, 0\right)^t$$
$$\qquad (5.61)$$

$$h_2(\delta q) = \frac{1}{2}\mathrm{d}^2 D(S)(\delta q, \delta q) = (1 - \epsilon)(\delta z_1 - \delta z_2)(\delta z_1 - (1 - \epsilon)^2 \delta z_2)(2\Gamma - \gamma)\gamma^2$$
$$\qquad (5.62)$$

$$h_2'(\delta q) = \frac{1}{2}\mathrm{d}^2 D'(S)(\delta q, \delta q) = (1 - \epsilon)(\delta z_1 - \delta z_2)(\delta y_2(\epsilon - 1) + \delta y_1)(2\Gamma - \gamma)^2\gamma^2.$$
$$\qquad (5.63)$$

Following [6] and [27], we study the projection of the differential equation $\dot{v} = H_2(v)$ on the sphere S^3. Let $w = v/\|v\|$ be this projection, it satisfies the differential equation

$$\dot{w} = \frac{1}{\|v\|^2}\left(\dot{v}\|v\| - v\frac{\langle v, \dot{v}\rangle}{\|v\|}\right) \qquad (5.64)$$

$$= \frac{H_2(v)}{\|v\|} - \frac{\langle v, H_2(v)\rangle}{\|v\|^3}v \qquad (5.65)$$

$$= \|v\|\big(H_2(w) - \langle w, H_2(w)\rangle w\big) \qquad (5.66)$$

so we are to study the following differential equation on the sphere S^3:

$$\dot{v} = H_2(v) - \langle v, H_2(v)\rangle v =: H_2^\pi(v). \qquad (5.67)$$

Invariants are related to the eigenvalues of the linearization of H_2^π at points where $H_2^\pi(v) = 0$. Those points are:

- lines of non-isolated singular points of H_2, that is vectors v such that $H_2(v) = 0$
- ray solutions, that is vectors ξ such that there exists $\lambda \in \mathbb{R}\backslash\{0\}$, $H_2(\xi) = \lambda\xi$.

We study the linearization of H_2^π in some neighborhood of these solutions in S^3.

Proposition 5.4. *The blow-up at point S has no ray solution, and two sets of non-isolated singularities:*

(1) *the projective plane $\delta z_1 = \delta z_2$;*
(2) *the projective line $\delta y_2 = (1-\epsilon)\delta y_1$, $\delta z_1 = (1-\epsilon)^2 \delta z_2$.*

In the first case, the Jacobian of the system is nilpotent. In the second case, it is diagonalizable with non-zero eigenvalues:

$$\frac{1}{2}\left(\bar{\delta y_2} + 1 \pm \sqrt{\bar{\delta y_2}^2 + (2\epsilon - 1)^2(\bar{\delta y_2} + 1) - 4(\epsilon - 1)^4 - 2\bar{\delta y_2} + 1}\right). \tag{5.68}$$

Proof. First we study ray solutions. Let ξ be a vector on a ray solution, such that

$$H_2(\xi) = \lambda\xi. \tag{5.69}$$

Let $\alpha\xi$ be another vector on the same line ($\alpha \in \mathbb{R}$), since H_2 is homogeneous with degree 2, one has

$$H_2(\alpha\xi) = \alpha^2 H_2(\xi) = \alpha^2\lambda\xi = \alpha\lambda(\alpha\xi). \tag{5.70}$$

So each line or ray solutions contains a unique ξ_0 such that $H_2(\xi_0) = \xi_0$.

A Gröbner basis of the system $\langle H_2(\delta q) - \delta q\rangle$ is given by $\{\delta y_1, \delta z_1, \delta y_2, \delta z_2\}$, so there is no non-trivial ray.

This can also be seen in the following way: let δq be a vector such that $H_2(\delta q) = \delta q$. By the structure of the vector $F(S)$, δq satisfies $\delta z_1 = \delta z_2$, and so $h_2(\delta q) = h_2'(\delta q) = 0$, so $H_2(\delta q) = 0$, and which, by hypothesis, implies that $\delta q = 0$.

We now consider non-isolated singular points of H_2, that is the zeroes of H_2. Since $F(S)$ and $G(S)$ are linearly independent, those points are exactly the zeroes of h_2 and h_2', as described in the statement of the proposition.

Then we study the linearization of H_2^π in some neighborhood of these solutions in S^3. First we consider vectors δq such that $\delta z_1 = \delta z_2$, we may perform the computations in the affine chart given by $\delta z_1 \neq 0$, with coordinates $\bar{\delta y_1} = \delta y_1/\delta z_1$, $\bar{\delta y_2} = \delta y_2/\delta z_1$, $\bar{\delta z_2} = \delta z_2/\delta z_1$. The differential equation becomes

$$\frac{\mathrm{d}}{\mathrm{d}t}\begin{pmatrix}\bar{\delta y_1}\\\bar{\delta y_2}\\\bar{\delta z_1}\end{pmatrix} = \delta z_2 \bar{C}(\bar{\delta y_1}, \bar{\delta y_2}, \bar{\delta z_1}) \tag{5.71}$$

with $\bar{C}$ a polynomial vector field of degree 3.

At $\bar{\delta z_1} = 1$, its Jacobian is nilpotent:

$$\begin{bmatrix}0 & 0 & (\epsilon-1)(\bar{\delta y_1}(\epsilon(\epsilon-1)-1) + \bar{\delta y_2}(1-\epsilon))(2\Gamma-\gamma)^2\gamma^3 \\ 0 & 0 & (\epsilon-1)(\bar{\delta y_1}(2\epsilon(\epsilon-2)+1) + \bar{\delta y_1}(\epsilon-1))(2\Gamma-\gamma)^2\gamma^3 \\ 0 & 0 & 0\end{bmatrix} \tag{5.72}$$

Then we consider vectors δq such that $\delta y_2 = (1-\epsilon)\delta y_1$, $\delta z_1 = (1-\epsilon)^2\delta z_2$. This time we use the chart $\delta z_2 \neq 0$ with coordinates $\bar{\delta y_1} = \delta y_1/\delta z_2$, $\bar{\delta y_2} = \delta y_2/\delta z_2$, $\bar{\delta z_1} = \delta z_1/\delta z_2$. As above, we compute the differential equation in this chart, linearize the resulting vector field, and evaluate this Jacobian at $\bar{\delta y_2} = (1-\epsilon)\bar{\delta y_1}$ and $\bar{\delta z_1} = (1-\epsilon)^2$. This matrix has rank 2 and is diagonalizable with non-zero eigenvalues:

$$\frac{1}{2}\left(\bar{\delta y_2} + 1 \pm \sqrt{\bar{\delta y_2}^2 + (2\epsilon - 1)^2(\bar{\delta y_2} + 1) - 4(\epsilon - 1)^4 - 2\bar{\delta y_2} + 1}\right). \tag{5.73}$$

$\square$

Cubic approximation at N. We perform the same study at the North pole N. With expression (5.58), we can verify that the quadratic component of $R(N)$ is 0. Indeed, $F(N) = 0$ and $\mathrm{d}^2 D'(N) = 0$.

Further differentiating along q, we obtain

$$H_3(\delta q) := \frac{1}{6}\mathrm{d}^3 f(N)(\delta q, \delta q, \delta q) \tag{5.74}$$

$$= \frac{1}{6}\left(3\mathrm{d}^2 D(N)(\delta q, \delta q)F(\delta q) - \mathrm{d}^3 D'(N)(\delta q, \delta q, \delta q)G(N)\right) \tag{5.75}$$

Note that since we centered the coordinates at the North pole, F is linear in q, so $\mathrm{d}F(q) = F$, and G is affine in q, so $\mathrm{d}G(q)$ is constant.

As in the previous subsection, we study the projection of the differential equation $\dot{v} = H_3(v)$ on the sphere S^3, and its equilibrium points, which form lines of non-isolated singular points and ray solutions.

Proposition 5.5. *The cubic blow-up at the North pole N, for admissible values of the parameters, has two sets of ray solutions:*

(1) *the projective line*

$$\begin{cases} \delta z_1 = \delta z_2 = 0 \\ (\epsilon - 1)\delta y_1 + \delta y_2 = \dfrac{1}{\Gamma(2\Gamma - \gamma)\sqrt{1 - \epsilon}}; \end{cases} \tag{5.76}$$

(2) *the quadric*

$$\begin{cases} \delta y_1 = \delta y_2 = 0 \\ ((\epsilon - 1)\delta z_1 - \delta z_2)^2 - (\epsilon - 2)\delta z_1 \delta z_2 = \dfrac{1}{\gamma^3(2\Gamma - \gamma)(1 - \epsilon)}. \end{cases} \tag{5.77}$$

and three sets of real non-isolated singularities:

(1) *the plane*

$$\begin{cases} \delta z_1 = \delta z_2 \\ \delta y_1(1 - \epsilon) = \delta y_2 \end{cases} \tag{5.78}$$

(2) *the plane*

$$\begin{cases} \delta y_2 = (1 - \epsilon)\delta y_1 \\ \delta z_2 = (1 - \epsilon)^2 \delta z_1 \end{cases} \tag{5.79}$$

(3) *the surface defined by*

$$\begin{cases} 0 = \Gamma(\epsilon - 1)(2\Gamma - \gamma)\delta y_1^2 + (2\Gamma - \gamma)\Gamma\delta y_1\delta y_2 + \gamma^2(\epsilon - 1)\delta z_1^2 - \gamma^2(\epsilon - 1)\delta z_1\delta z_2 \\ 0 = \Gamma(\epsilon - 1)(2\Gamma - \gamma)\delta y_1\delta y_2 - \gamma^2\delta z_1\delta z_2 + (2\Gamma - \gamma)\Gamma\delta y_2^2 + \gamma^2\delta z_2^2 \\ 0 = \delta y_1\delta z_2 + (\epsilon - 1)\delta y_2\delta z_1. \end{cases} \tag{5.80}$$

For points on the line (5.76), the linearization of H_3^π is diagonal: the vectors $(1, 0, 0)$ and $(0, 0, 1)$ are eigenvectors, with the same eigenvalue, and the vector $(0, 0, 1)$ is in the kernel.

For isolated singularities satisfying (5.78), the matrix is not diagonalizable, its Jordan form has the following structure:

$$\begin{bmatrix} 0 & 0 & 0 \\ 0 & * & 1 \\ 0 & 0 & * \end{bmatrix} \tag{5.81}$$

For isolated singularities satisfying (5.79), the matrix is diagonalizable with 3 non-zero eigenvalues.

Proof. First we study ray solutions. Let ξ be a vector on a ray solution, such that

$$H_3(\xi) = \lambda \xi. \tag{5.82}$$

Let $\alpha\xi$ be another vector on the same line ($\alpha \in \mathbb{R}$), one has

$$H_3(\alpha\xi) = \alpha^3 H_3(\xi) = \alpha^3 \lambda \xi = \alpha^2 \lambda(\alpha\xi). \tag{5.83}$$

So unlike in the quadratic case, a line of ray solutions contains 2 vectors ξ_1, ξ_2 such that either $H_3(\xi_1) = H_3(\xi_2) = 1$ or $H_3(\xi_1) = H_3(\xi_2) = -1$.

In order to study ray solutions, we compute a Gröbner basis of the system $H_3(\delta q) - \iota \delta q = 0, \iota^2 = 1$, for an order eliminating α. We find that the basis contains

$$\{\delta y_1 \delta z_1, \delta y_1 \delta z_2, \delta y_2 \delta z_1, \delta y_2 \delta z_2\} \tag{5.84}$$

so either $\delta y_1 = \delta y_2 = 0$ or $\delta z_1 = \delta z_2 = 0$.

If $\delta z_1 = \delta z_2 = 0$, computing a new Gröbner basis of the system, saturating with $\Gamma - \gamma$ and δy_1 shows that δy_1 and δy_2 must satisfy

$$\left(\Gamma^2(\epsilon - 1)(2\Gamma - \gamma)^2 \left((\epsilon - 1)\delta y_1 + \delta y_2\right)^2 \right)^2 - 1 = 0. \tag{5.85}$$

Since $\epsilon - 1 < 0$, $2\Gamma - \gamma > 0$ and $\Gamma > 0$, this defines 2 lines of real solutions given by

$$(\epsilon - 1)\delta y_1 + \delta y_2 = \pm \frac{1}{\Gamma(2\Gamma - \gamma)\sqrt{1 - \epsilon}} \tag{5.86}$$

Those lines are equivalent in the projective space: each line of ray-solutions contains a vector in both lines.

If $\delta y_1 = \delta y_2 = 0$, the same technique shows that δz_1 and δz_2 must satisfy

$$\left(\gamma^3(2\Gamma - \gamma)(\epsilon - 1)\left(((\epsilon - 1)\delta z_1 - \delta z_2)^2 - (\epsilon - 2)\delta z_1 \delta z_2\right) \right)^2 - 1 = 0, \tag{5.87}$$

which defines 1 quadric

$$((\epsilon - 1)\delta z_1 - \delta z_2)^2 - (\epsilon - 2)\delta z_1 \delta z_2 = \frac{1}{\gamma^3(2\Gamma - \gamma)(1 - \epsilon)}. \tag{5.88}$$

We now consider non-isolated singularities, that is zeroes of H_3. To this end, we compute a Gröbner basis of the system $H_3(\delta q) = 0$, saturating by $\gamma - \Gamma$, γ, Γ, $\epsilon - 1$ and $2\Gamma - \gamma$. Factoring the results, it appears that the solutions split into 5 cases:

(1) $\delta z_1 = \delta z_2$
(2) $\delta z_1 = -\delta z_2$
(3) $\delta z_1 = 0$
(4) $\delta z_2 = (1 - \epsilon)^2 \delta z_1$
(5) otherwise.

In the case 1, a Gröbner basis is given by

$$\begin{cases} \delta y_1(\delta y_1(\epsilon - 1) + \delta y_2)^2 \\ \delta y_2(\delta y_1(\epsilon - 1) + \delta y_2)^2 \\ \delta z_2(\delta y_1(\epsilon - 1) + \delta y_2)^2 \\ \delta z_1 - \delta z_2 \end{cases} \tag{5.89}$$

and the solutions form the plane (5.78).

In the case 2, saturating by $\delta z_1 - \delta z_2$, a Gröbner basis is given by

$$\begin{cases} \delta y_1 + (1 - \epsilon)\delta y_2 \\ \delta z_1 + \delta z_2 \\ \Gamma(\epsilon^2 - 2\epsilon + 2)(2\gamma - \gamma)\delta y_2^2 + 2\gamma^2\delta z_2^2 \end{cases} \tag{5.90}$$

which has no real non-zero solution for admissible values of the parameters.

In the case 3, saturating by $\delta z_1 - \delta z_2$ and $\delta z_1 + \delta z_2$, a Gröbner basis is given by

$$\left\{ \delta y_1, \delta z_1, (2\Gamma - \gamma)\Gamma\delta y_2^2 + \gamma^2\delta z_2^2 \right\} \tag{5.91}$$

which has no real non-zero solution for admissible values of the parameters.

In the case 4, saturating by $\delta z_1 \pm \delta z_2$ and δz_1, a Gröbner basis is given by

$$\left\{ \delta y_1\delta z_2 + (\epsilon - 1)\delta y_2\delta z_1, \delta y_2 + (\epsilon - 1)\delta y_1, \delta z_2 - (\epsilon - 1)^2\delta z_1 \right\} \tag{5.92}$$

and the solutions form the plane (5.79).

Finally, for the case 5, we compute a Gröbner basis, saturating by all the previous conditions. This basis is

$$\begin{cases} \Gamma(\epsilon - 1)(2\Gamma - \gamma)\delta y_1^2 + (2\Gamma - \gamma)\Gamma\delta y_1\delta y_2 + \gamma^2(\epsilon - 1)\delta z_1^2 - \gamma^2(\epsilon - 1)\delta z_1\delta z_2 \\ \Gamma(\epsilon - 1)(2\Gamma - \gamma)\delta y_1\delta y_2 - \gamma^2\delta z_1\delta z_2 + (2\Gamma - \gamma)\Gamma\delta y_2^2 + \gamma^2\delta z_2^2 \\ \delta y_1\delta z_2 + (\epsilon - 1)\delta y_2\delta z_1 \\ \left(\Gamma(2\Gamma - \gamma)(\epsilon - 1)^2\delta y_2^2 + \delta z_2^2\gamma^2\right)\delta z_1 - (2\Gamma - \gamma)\Gamma\delta z_2\delta y_2^2 - \gamma^2\delta z_2^3 \end{cases} \tag{5.93}$$

The fourth polynomial is a combination of the other 3, and the solutions form the surface (5.80).

For the second part of the proposition, as in the quadratic case, we study the linearization of $H_3^\pi : \dot{v} = H_3(v) - \langle v, H_3(v) \rangle v$. In the affine chart with $\delta y_1 \neq 0$, with coordinates $\bar{\delta z_1} = \delta z_1/\delta y_1$, $\bar{\delta y_2} = \delta y_2/\delta y_1$ and $\bar{\delta z_2} = \delta z_2/\delta y_1$, the differential equation $\dot{v} = H_3(v)$ becomes

$$\frac{\mathrm{d}}{\mathrm{d}t}\begin{pmatrix} \bar{\delta z_1} \\ \bar{\delta y_2} \\ \bar{\delta z_2} \end{pmatrix} = \delta y_1^2\bar{Q}(\bar{\delta z_1}, \bar{\delta y_2}, \bar{\delta z_2}) \tag{5.94}$$

with $\bar{Q}$ a polynomial vector field of degree 4. In this chart, H_3^π becomes

$$\dot{v} = \bar{Q}(v). \tag{5.95}$$

We conclude by evaluating the Jacobian of $\bar{Q}$ at the relevant points.   □

5.3.2. *General case.*

Singularities of $\{\mathcal{D} = H_G = \{H_G, H_F\} = 0\}$.

Proposition 5.6. *The set of singularities of $\{\mathcal{D} = H_G = \{H_G, H_F\} = 0\}$ is given, generically on authorized values of γ, Γ, by*

(1) *the plane $z_1 = z_2 = z_S$;*
(2) *the line $z_1 = z_2$, $y_1 = y_2 = 0$;*
(3) *an irreducible variety of dimension 5.*

If $\gamma = \Gamma$, solution 2 becomes a surface defined by $z_1 = z_2$, $y_2 = (1 - \epsilon)y_1$.

Proof. By definition of $\mathcal{D} = \{\{H_G, H_F\}, H_G\}$, we want to study the zeroes of

$$\begin{cases} 0 & = p \cdot G \\ 0 & = p \cdot [G, F] \\ 0 & = p \cdot [[G, F], G] \end{cases} \tag{$\mathcal{D}$}$$

The singularities of this variety is the set of points at which the matrix

$$\begin{bmatrix} G & [G, F] & [[G, F], G] \end{bmatrix} \tag{5.96}$$

has rank at most 2.

We encode that with the incidence variety

$$\begin{bmatrix} G & [G, F] & [[G, F], G] \\ v_1 & v_2 & v_3 \end{bmatrix} \cdot \begin{bmatrix} L_1 \\ L_2 \\ L_3 \end{bmatrix} = \begin{bmatrix} 0 \\ 0 \\ 0 \\ 1 \end{bmatrix} \tag{5.97}$$

with new variables $\mathbf{L} = L_1, L_2, L_3$ and random numbers v_1, v_2, v_3. This gives us a system of 4 polynomial equations in the 10 unknowns $y_1, z_1, y_2, z_2, L_1, L_2, L_3, \Gamma, \gamma, \epsilon$. We eliminate L_1, L_2, L_3 from the ideal in order to recover the projection, and we saturate by $1 - \epsilon$.

We then compute a Gröbner basis for the elimination order $y_1 > y_2 > z_1 > z_2 \gg \gamma > \Gamma > \epsilon$, this basis contains 10 polynomials, some of which have factors with multiplicity greater than 1 or are divisible by $1 - \epsilon$ or γ. We take the square-free form of this basis, and we saturate by $1 - \epsilon$ and γ before computing a new Gröbner basis for the same order. The result is a set of 11 polynomials which includes

$$(z_1 - z_2)\left((\epsilon - 1)P_{z_2}y_1 + P_{z_1}y_2\right). \tag{5.98}$$

First, we add $z_1 - z_2$ to the ideal. Once again, we compute a Gröbner basis for the elimination order $y_1 > y_2 > z_1 > z_2 \gg \gamma > \Gamma > \epsilon$, take its square-free form, and recompute a Gröbner basis. The result contains the polynomial

$$P_{z_2}P_{y_2}. \tag{5.99}$$

The solutions decompose into 2 algebraic sets, defined by

$$z_1 = z_2 = z_S = \frac{2\Gamma - \gamma}{2\Gamma - 2\gamma} \tag{5.100}$$

and (adding $(\epsilon - 1)y_1 + y_2$ to the ideal and saturating by P_{z_2}, ϵ and $\epsilon - 2$)

$$\begin{cases} 0 & = y_1(\Gamma - \gamma) \\ 0 & = y_2(\Gamma - \gamma) \\ 0 & = P_{y_2} = (\epsilon - 1)y_1 + y_2 \\ 0 & = z_1 - z_2. \end{cases} \tag{5.101}$$

The latter is generically (if $\Gamma \neq \gamma$) defined by

$$\begin{cases} y_1 = y_2 = 0 \\ z_1 = z_2 \end{cases} \tag{5.102}$$

or if $\Gamma = \gamma$ (that is if the spin we consider is water), by

$$\begin{cases} y_1 = \frac{y_2}{\epsilon - 1} \\ z_1 = z_2. \end{cases} \tag{5.103}$$

Then, starting again with the whole ideal, we add $(\epsilon - 1)P_{z_2}y_1 + P_{z_1}y_2$ to the ideal and saturate by $z_1 - z_2$. The result, generically on $(\Gamma, \gamma, \epsilon)$, is an irreducible surface. □

Locus of $\{\mathcal{D} = \mathcal{D}' = H_G = \{H_G, H_F\} = 0\}$**.**

Proposition 5.7. *The solutions form the union of the hyperplane defined by*

$$z_1 = z_2 \tag{5.104}$$

and the hypersurface

$$y_1 = -\frac{y_2 P_{z_1}}{(\epsilon - 1) P_{z_2}}. \tag{5.105}$$

Proof. Points such that $\{\mathcal{D} = \mathcal{D}' = H_G = \{H_G, H_F\} = 0\}$ satisfy

$$\begin{cases} 0 & = p \cdot G \\ 0 & = p \cdot [G, F] \\ 0 & = p \cdot [[G, F], G] \\ 0 & = p \cdot [[G, F], F] \end{cases} \tag{5.106}$$

The projection of these points onto the space (y_1, z_1, y_2, z_2) is given by the vanishing of the determinant Δ', defined as

$$\Delta' = \det \begin{bmatrix} G & [G, F] & [[G, F], G] & [[G, F], F] \\ (1 - \epsilon)G & [(1 - \epsilon)G, F] & [[(1 - \epsilon)G, F], (1 - \epsilon)G] & [[(1 - \epsilon)G, F], F] \end{bmatrix} \tag{5.107}$$

$$= (1 - \epsilon)^2 \det \begin{bmatrix} G & [G, F] & [[G, F], G] & [[G, F], F] \\ G & [G, F] & (1 - \epsilon)[[G, F], G] & [[G, F], F]. \end{bmatrix} \tag{5.108}$$

This determinant factors as

$$-2(\epsilon - 1)^2(2\Gamma - 1)(\Gamma - 1)(z_1 - z_2)\left[(\epsilon - 1)P_{z_2}y_1 + P_{z_1}y_2\right] \tag{5.109}$$

□

Equilibrium positions.

Lemma 5.8. *All equilibrium points of $\dot{Z} = \mathcal{D}\vec{H}_F - \mathcal{D}'\vec{H}_G$ satisfying $H_G = \{H_G, H_F\} = 0$ are contained in $\{\mathcal{D} = \mathcal{D}' = 0\}$.*

Proof. Recall that $\vec{H}_F$ is defined as

$$\vec{H}_F = \begin{bmatrix} \frac{\partial H_F}{\partial p} \\ -\frac{\partial F}{\partial q} \end{bmatrix} = \begin{bmatrix} F \\ -p \cdot \frac{\partial H_F}{\partial q} \end{bmatrix} \tag{5.110}$$

and $\vec{H}_G$ is defined in the same way. Let $z = (q, p)$ be a point such that

$$\mathcal{D}(z)\vec{H}_F(z) - \mathcal{D}'(z)\vec{H}_G(z) = 0, \tag{5.111}$$

by looking at the first 4 components of this system, we see that the vectors $F(q)$ and $G(q)$ are colinear.

Introduce new variables $X_{\mathcal{D}}$ and $X_{\mathcal{D}'}$ and consider the ideal generated by

- $X_{\mathcal{D}}F(q) - X_{\mathcal{D}'}G(q) = 0$
- $H_G(z) = \{H_G, H_F\}(z) = 0$
- $\mathcal{D}(z)\vec{H}_F(z) - \mathcal{D}'(z)\vec{H}_G(z) = 0$

saturated by $X_{\mathcal{D}}$ and $X_{\mathcal{D}'}$. Computing a Gröbner basis of this ideal (for any order) yields that this ideal is actually $\langle 1 \rangle$, and so the associated system has no solution.

Hence, at an equilibrium point, either $\mathcal{D}(z)$ or $\mathcal{D}'(z)$ has to be 0. Since both O (the center of the Bloch ball) and N (the north pole) are on the hyperplane $z_1 = z_2 = 0$, which is contained in $\{\mathcal{D} = \mathcal{D}' = 0\}$, we may assume that the point z is neither O nor N. Hence, $F(z)$ and $G(z)$ are non-zero, and so $\mathcal{D}(z) = \mathcal{D}'(z) = 0$. $\quad\square$

Eigenvalues of the linearization. We consider the eigenvalue decomposition of the matrix

$$\mathcal{A} = \text{Jac}(\mathcal{D}\vec{H}_F - \mathcal{D}'\vec{H}_G) \tag{5.112}$$

on equilibrium point, given as the union of points satisfying Eq. (5.104) and (5.105).
Solutions of Eq. (5.104). If $z_1 = z_2$, the matrix $\mathcal{A}$ has rank 2, and its characteristic polynomial is

$$T^6 \left(T^2 - \frac{\epsilon(\epsilon - 1)(\epsilon - 2)\left(8(\Gamma - \gamma)^2 P_{y_1} y_1 y_2 + P_{z_2}(2 P_{z_2} - \gamma)P_{y_2}\right)}{2P_{y_1}(\Gamma - \gamma)y_1} T \right.$$
$$\left. + \left(\frac{(\epsilon - 1)\gamma P_{y_1}(2\Gamma - \gamma)}{y_1} \right)^2 \right) \tag{5.113}$$

Solutions of Eq. (5.105). If $y_2 = -\frac{y_2 p_{z_1}}{(\epsilon - 1)p_{z_2}}$, the matrix $\mathcal{A}$ has rank 2, and its characteristic polynomial is

$$T^6 \left(T^2 - 4\epsilon y_2(\epsilon - 1)(\epsilon - 2)(\Gamma - \gamma)T + \left(\frac{2\gamma(z_1 - z_2)(\epsilon - 1)^2(2\Gamma - \gamma)(\Gamma - \gamma)}{p_{z_1}} \right)^2 \right). \tag{5.114}$$

The discriminant of the degree 2 factor factors as

$$\frac{16(\Gamma - \gamma)^2(\epsilon - 1)^2 \left(a_6(z_1, y_2) - b_6(z_1, z_2)\right)\left(a_6(z_1, y_2) + b_6(z_1, z_2)\right)}{p_{z_1}^2} \tag{5.115}$$

with

$$a_6(z_1, y_2) = \epsilon(\epsilon - 2)P_{z_1}y_2 \qquad (5.116)$$

$$b_6(z_1, z_2) = (2\Gamma - \gamma)(\epsilon - 1)\gamma(z_1 - z_2) \qquad (5.117)$$

which induces the following classification of the eigenvalues of $\mathcal{A}$:

- if $|a(z_1, y_2)| > |b(z_1, z_2)|$: 2 single real eigenvalues;
- if $|a(z_1, y_2)| = |b(z_1, z_2)|$: 1 double real eigenvalue;
- if $|a(z_1, y_2)| < |b(z_1, z_2)|$: 2 single complex eigenvalues.

6. Conclusion

In this article we made a complete use of the state of the art in geometric, symbolic and numeric techniques to analyze the problem of saturating a pair of spins in relation with the B_1-inhomogeneities, that is inhomogeneities of the applied RF-field. We extend the results in many directions. First of all, the time minimal syntheses for a single spin are classified, taking into account the relaxation parameters and the control bounds. For a pair of spins, the crucial theoretical problem is to classify the singularities of the extremal flow. This is realized using symbolic computations based on Gröbner basis to compute the singularities and linear or quadratic, cubic approximations of some crucial frame points. This is not sufficient to make a topological classification of the behaviours, since Grobman-Hartman cannot be applied in general for non isolated singularities, see [6]. Nevertheless numerical methods using continuation techniques can be used to analyze the singularities. One feature of the problem is the existence of many local optima and applications of LMI techniques are particularly important to compare the different local optima obtained using direct or indirect numerical schemes implemented in the `Bocop` and `HamPath` software. Hence, we believe that this article complete in many directions the results and techniques obtained in previous articles. It is a relevant step in the problem of determining the cartography of the global optima with respect to the relaxation parameters in the (ideal) contrast problem in MRI and to provide substantial improvements in existing software in MRI.

Also in the contrast of geometric optimal control it is a significant step to handle complex 4-D problems.

References

[1] E. Allgower & K. Georg, <u>Introduction to numerical continuation methods</u>, vol. **45** of Classics in Applied Mathematics, Soc. for Industrial and Applied Math., Philadelphia, PA, USA (2003), xxvi+388

[2] J.T. Betts <u>Practical methods for optimal control using nonlinear programming</u>, Society for Industrial and Applied Mathematics (SIAM), Philadelphia (2001)

[3] F. J. Bonnans, P. Martinon & V. Grélard. <u>Bocop - A collection of examples</u>, Technical report, INRIA (2012) RR-8053

[4] B. Bonnard, J.-B. Caillau & E. Trélat, <u>Second order optimality conditions in the smooth case and applications in optimal control</u>, ESAIM: COCV **13**, no. 2 (2007), 207–236

[5] B. Bonnard & M. Chyba, <u>Singular trajectories and their role in control theory</u>, vol **40** of Mathematics & Applications, Springer-Verlag, Berlin (2003), xvi+357

[6] B. Bonnard, M. Chyba, A. Jacquemard & J. Marriott, <u>Algebraic geometric classification of the singular flow in the contrast imaging problem in nuclear magnetic resonance. Mathematical Control and Related Fields-AIMS</u>, Special issue in the honor of Bernard Bonnard. Part II., **3** no. 4 (2013), 397–432

[7] B. Bonnard, M. Chyba & J. Marriott, <u>Singular Trajectories and the Contrast Imaging Problem in Nuclear Magnetic Resonance</u>, SIAM J. Control Optim., **51** no. 2 (2013), 1325–1349

[8] B. Bonnard, M. Claeys, O. Cots & P. Martinon, <u>Geometric and numerical methods in the contrast imaging problem in nuclear magnetic resonance</u>, Acta Appl. Math., **135** no. 1 (2014), 5–45

[9] B. Bonnard & O. Cots, <u>Geometric numerical methods and results in the control imaging problem in nuclear magnetic resonance</u>, Math. Models Methods Appl. Sci., **24** no. 1 (2012), 187–212

[10] B. Bonnard, O. Cots, J.-C. Faugère, A. Jacquemard, J. Rouot, M. Safey El Din & T. Verron, <u>Algebraic-geometric techniques for the feedback classification and robustness of the optimal control of a pair of Bloch equations with application to Magnetic Resonance Imaging</u>, HAL Id : hal-01556806 (2017) `http://hal.inria.fr/hal-01556806`

[11] B. Bonnard, O. Cots, S. Glaser, M. Lapert, D. Sugny & Y. Zhang, <u>Geometric optimal control of the contrast imaging problem in nuclear magnetic resonance</u>, IEEE Trans. Automat. Control, **57** no. 8 (2012), 1957–1969

[12] B. Bonnard & I. Kupka, <u>Théorie des singularités de l'application entrée/sortie et optimalité des trajectoires singulières dans le problème du temps minimal</u>, Forum Math., **5** no. 2 (1993), 111–159

[13] U. Boscain & B. Piccoli, <u>Optimal Syntheses for Control Systems on 2-D Manifolds</u>, Springer SMAI, **43** (2004)

[14] R. Bulirsch and J. Stoer, <u>Introduction to numerical analysis</u>, vol.**12** of <u>Texts in Applied Mathematics</u>, Springer-Verlag, New York, 2nd edition, 1993, xvi+744

[15] J.-B. Caillau, O. Cots & J. Gergaud, <u>Differential continuation for regular optimal control problems</u>, Optimization Methods and Software, **27** no. 2 (2011), 177–196

[16] M. Claeys, J. Daafouz, and D. Henrion. <u>Modal occupation measures and {LMI} relaxations for nonlinear switched systems control</u>, Automatica, **64** (2016), 143–154

[17] S. Conolly, D. Nishimura & A. Macovski, <u>Optimal control solutions to the magnetic resonance selective excitation problem</u>, IEEE Trans. Med. Imaging, **5** no. 2 (1986), 106–115

[18] M. Gerdts, <u>Optimal Control of ODEs and DAEs</u>, ed. De Gruyter, Berlin (2011)

[19] D. Henrion, J. B. Lasserre & J. Löfberg, <u>GloptiPoly 3: Moments, Optimization and Semidefinite Programming</u>, Optim. Methods and Software, **24** no. 4-5 (2009), 761–779

[20] A. J. Krener, <u>The high order maximal principle and its application to singular extremals</u>, SIAM J. Control Optim., **15** no. 2 (1977), 256–293

[21] I. Kupka, <u>Geometric theory of extremals in optimal control problems. I. The fold and Maxwell case</u>, Trans. Amer. Math. Soc., **299** no. 1 (1987), 225–243

[22] M. Lapert, Y. Zhang, M. Braun, S. J. Glaser & D. Sugny, <u>Singular extremals for the time-optimal control of dissipative spin 1/2 particles</u>, Phys. Rev. Lett., **104** no. 2 (2010), 083001

[23] M. Lapert, Y. Zhang, M. A. Janich, S. J. Glaser, and D. Sugny, <u>Exploring the physical limits of saturation contrast in magnetic resonance imaging</u>, Sci. Rep., **589** (2012)

[24] J.-B. Lasserre, <u>Moments, Positive Polynomials and Their Applications</u>, Imperial College Press, London (2009)

[25] J.-B. Lasserre, D. Henrion, C. Prieur, and E. Trélat. <u>Nonlinear optimal control via occupation measures and LMI-relaxations</u>, SIAM J. Control Optim., **47** no. 4 (2008), 1643–1666

[26] M. H. Levitt, <u>Spin dynamics: Basics of Nuclear Magnetic Resonance</u> John Wiley & Sons, New York-London-Sydney (2008)

[27] L. Markus, <u>Quadratic differential equations and non-associative algebras</u>, Princeton Univ. Press, Princeton, N.J. (1960), 185–213

[28] H. Maurer, <u>Numerical solution of singular control problems using multiple shooting techniques</u>, J. Optim. Theory Appl., **18** no. 2 (1976), 235–257

[29] ApS Mosek. <u>The mosek optimization toolbox for matlab manual</u>, Version 7.1 Revision 28 (2015)

[30] J. Nocedal and S. J. Wright, <u>Numerical optimization</u>, Springer-Verlag, New York (1999)

[31] L. S. Pontryagin, V. G. Boltyanskiĭ, R. V. Gamkrelidze & E. F. Mishchenko, <u>The Mathematical Theory of Optimal Processes</u>, Translated from the Russian by K. N. Trirogoff, edited by L. W. Neustadt, Interscience Publishers John Wiley & Sons, Inc., New York-London (1962)

[32] M. Putinar, Positive polynomials on compact semi-algebraic sets, Indiana Univ. Math. J., **42** no. 3 (1993), 969–984

[33] H. Schättler, The local structure of time-optimal trajectories in dimension three under generic conditions, SIAM J. Contr. Opt., **26** no. 4 (1988), 899–918

[34] H. J. Sussmann, Time-optimal control in the plane, in Feedback control of linear and nonlinear systems, (Bielefeld/Rome, 1981), vol. 39 of Lecture Notes in Control and Inform. Sci., Springer, Berlin (1982), 244–260

[35] H.J. Sussmann, Regular synthesis for time-optimal control of single-input real-analytic systems in the plane, SIAM J. Control and Opt. **25** no. 5 (1987), 1145–1162

[36] E. Van Reeth, H. Ratiney, M. Tesch, D. Grenier, O. Beuf, S. J. Glaser & D. Sugny, Optimal control design of preparation pulses for contrast optimization in MRI, J. Magn. Reson., **279** (2017), 39–50.

Institut de Mathématiques de Bourgogne, Université de Bourgogne, 9 avenue Alain Savary, 21078 Dijon France and INRIA 2004 route des Lucioles F-06902 Sophia Antipolis
  E-mail address: `bernard.bonnard@u-bourgogne.fr`

Toulouse Univ., INP-ENSEEIHT-IRIT UMR CNRS 5505, 2 rue Camichel, 31071 Toulouse, France
  E-mail address: `olivier.cots@irit.fr`

EPF:École d'Ingénieur-e-s, 2 Rue F Sastre, 10430 Rosières-prés-Troyes, France
  E-mail address: `jeremy.rouot@epf.fr`

Institute for Algebra, Johannes Kepler University, 4040 Linz, Austria
  E-mail address: `thibaut.verron@jku.at`